Robust passivity-based continuous sliding-mode control for under-actuated nonlinear wing sections

Xiaojun Wei and John E Mottershead

Centre for Engineering Dynamics, University of Liverpool,
Liverpool L69 3GH, United Kingdom

j.e.mottershead@liverpool.ac.uk

Abstract

The stability of an under-actuated nonlinear aeroelastic wing section is addressed using a robust passivity-based continuous sliding-mode control approach. The controller is shown to be capable of stabilising the system in the presence of large matched and mismatched uncertainties and large input disturbance. It is demonstrated in theory that within known bounds on the input disturbance and nonlinearity uncertainty, the controller is able to stabilise the system globally. A numerical example, based on the Texas A&M University experimental rig, is used to demonstrate the stabilisation of the system with a fully-developed limit cycle oscillation and a flap deflection limited to 20 degrees. This is of practical interest because it shows that the system is at least stabilised locally, whereas global stability is a concept limited to theoretical studies and is impossible to demonstrate in practice.

Keywords: Robust passivity-based control; Sliding-mode control; Matched uncertainty; Mismatched uncertainty; Input disturbance; Under-actuated nonlinear wing section

1. Introduction

Structural nonlinearity is encountered quite often in modern aircraft and is likely to be found more frequently in the future as increasingly lightweight and more flexible structural materials are introduced. The resultant nonlinear flutter, typically limit cycle oscillation (LCO), is already encountered in military and civil aircraft [1-6] leading to a reduced aeroelastic performance, structural fatigue and even failure of the vehicle. Never-the-less the requirements of next-generation flight vehicles place increasing and contradictory demands on designers, typically greater structural flexibility, improved manoeuvrability and greater operational safety in severe environmental conditions [7]. Hence, active nonlinear flutter suppression becomes increasingly important in ensuring the safety and efficiency of future aircraft [8] and presents intellectual challenges that have attracted the interest of researchers in aerospace and control communities for more than three decades.

In the control community, mechanical systems which have fewer independent actuators than degrees of freedom to be controlled are known as under-actuated mechanical systems [9]. The control design of under-actuated aeroelastic systems is of importance, firstly for reasons of actuator failure and the need to rely on fewer actuators. Secondly, under-actuation might be motivated by weight and cost constraints imposed on next-generation flight vehicles. A typical under-actuated aeroelastic system is a two-dimensional nonlinear wing section with a

single control surface in incompressible flow, which is the control objective of the present paper.

Linear control techniques, namely pole placement [10], linear quadratic regulation [11] and linear quadratic Gaussian methods [12], have been employed for nonlinear flutter suppression in two-dimensional wing sections with a single control surface, but with limited success [11]. Hence, nonlinear control methodologies are required for flutter suppression in nonlinear aeroelastic systems, e.g. Ko et al. [13, 14] employed feedback linearisation techniques to control a prototypical wing section with torsional nonlinearity.

In practice, unmodelled dynamics, parameter uncertainty and external disturbances in nonlinear control systems are unavoidable. Adaptive and robust control are two of the leading techniques for uncertainty compensation. Several adaptive control algorithms have been proposed for control of typical wing sections with structural nonlinearity using a single trailing-edge control, namely adaptive feedback linearisation [15], structured model reference adaptive control [16], output-feedback adaptive control [17] and backstepping-based adaptive control [18]. Alternatively, Lyapunov-based robust control is considered in [19] for an under-actuated nonlinear wing section. A robust controller in the form of state feedback control in conjunction with a proportional-integral observer, is used for active flutter suppression of a nonlinear two-dimensional wing-flap system [20]. Usually, robust constant-gain feedback control allows for the handling of small uncertainties, while adaptive control is applicable for a wider range of parameter variation but is sensitive to unstructured uncertainty [9].

In recent years, sliding-mode control, a variable-structure controller, has been developed for control design of dynamic systems under uncertainty conditions. The idea of sliding-mode control is to design a high-frequency switching (discontinuous) control law to drive the system onto a specified sliding surface in state space and maintain it there for all subsequent time. The resultant sliding mode is claimed to be insensitive to model uncertainties and disturbances which do not steer the system away from the specified surface. The advantage of sliding-mode control is its tolerance of large matched uncertainty and large input disturbance.

Continuous sliding-mode control [21], second-order sliding-mode control [22, 23] and dynamic sliding-mode control [24] have been applied to suppress flutter instability in two-dimensional nonlinear wing sections with leading- and trailing-edge control surfaces, i.e. fully actuated aeroelastic systems. Very little research appears to have been carried out on the use of sliding-mode control for under-actuated aeroelastic systems. Examples include the robust control of supersonic three degree-of-freedom aerofoils using sliding-mode control [25]. Gujjula and Singh [26] designed a discontinuous sliding-mode controller for the pitch angle trajectory control of an unsteady aeroelastic system with a single control surface. Of course control of under-actuated systems is more complicated than the control of fully-actuated ones, requiring the consideration of global stability and the presence of mismatched uncertainty.

Usually, for under-actuated systems, local asymptotic stability can be achieved by existing nonlinear control techniques. However, global asymptotic stabilisation for tracking control of under-actuated mechanical systems is considered to be extremely challenging [9, 27]. For example, by using feedback linearisation techniques, the stability of the zero dynamics only

guarantees local stability of the system, global asymptotical stability can only be achieved if the internal dynamics is input-to-state stable [28]. Under-actuated nonlinear aeroelastic systems are even more complicated owing to the intrinsic uncertainty.

The main contribution of this paper is to develop a robust passivity-based continuous sliding-mode control approach, which in theory can globally stabilise all the degrees of freedom of an under-actuated nonlinear prototypical wing section with matched and mismatched uncertainty and input disturbance - practical limitations mean that stability can only be demonstrated locally, as will be shown in a numerical case study. A robust passivity-based control method is used for the design of globally asymptotically (or exponentially) stable nonlinear sliding surfaces. Moreover, a proposed continuous sliding-mode control is able to alleviate the chattering which occurs in the process of discontinuous sliding-mode control. The sufficient conditions for global asymptotic stability and global stability of under-actuated two-degree-of-freedom nonlinear aeroelastic systems are provided. Compared with feedback linearisation or adaptive feedback linearisation, the proposed method relaxes the requirements for global asymptotical stability because it does not require the internal dynamics to be input-to-state stable. Bounds must be specified on the nonlinear uncertainty, but knowledge of the structure of the nonlinearity is not needed.

The nonlinear aeroelastic model is presented in Section 2 of this paper. In Section 3, the cascaded structure of the under-actuated aeroelastic model is obtained by an appropriate coordinate transformation to facilitate the control design. Bounded nonlinear pitch-stiffness uncertainty is considered, resulting in both matched and unmatched uncertainty terms. The proposed controller is designed in Section 4 to be robust not only to these uncertainties but also to control input disturbances. A numerical case study is used to illustrate the working of the proposed method. The research described in this paper form a basis for further work on passivity-based sliding-mode controllers to handle not only structural uncertainties but also uncertain aerodynamic parameters and to include the dynamics of the actuator in the formulation.

2. Nonlinear aeroelastic model

The under-actuated nonlinear system in question takes the form of a generic two-dimensional wing section with trailing-edge control surface, as depicted in Fig. 1. This example was used previously for classic aeroelastic analysis and control design [16]. The wing section with chord $c = 2b$ and span s_w is supported by a linear spring with stiffness K_h in plunge and a nonlinear torsional spring with stiffness $K_\alpha(\alpha)$ in pitch. The springs are attached at a distance $a_h b$ from the midchord, defining the elastic axis. The centre of mass is at a distance $r_{cg} = x_\alpha b$ from the elastic axis.

The governing equations of motion of the model were given by Ko et al. [16] ,

$$m_T \ddot{h} + m_W x_\alpha b \ddot{\alpha} + C_h \dot{h} + K_h h = -L \tag{1}$$

$$m_W x_\alpha b\ddot{h} + I_\alpha \ddot{\alpha} + C_\alpha \dot{\alpha} + K_\alpha(\alpha)\alpha = M \tag{2}$$

where h and α denote plunge and pitch displacements respectively; m_T is the total mass of wing and its supporting structure; m_W is the mass of wing; I_α is the mass moment of inertia about the elastic axis; and C_h and C_α are structural damping coefficients in plunge and pitch respectively.

L and M are the aerodynamic lift and moment about the elastic axis. Quasi-steady aerodynamic forces [29] are employed such that,

$$L = \rho V^2 b s_W C_{L_\alpha}\left(\alpha + \frac{\dot{h}}{V} + \left(\frac{1}{2} - a_h\right) b\frac{\dot{\alpha}}{V}\right) + \rho V^2 b s_W C_{L_\beta}\beta \tag{3}$$

$$M = \rho V^2 b^2 s_W C_{M_\alpha}\left(\alpha + \frac{\dot{h}}{V} + \left(\frac{1}{2} - a_h\right) b\frac{\dot{\alpha}}{V}\right) + \rho V^2 b^2 s_W C_{M_\beta}\beta \tag{4}$$

where ρ is the air density; V is free airflow speed; β is the trailing-edge control surface deflection; C_{L_α} and C_{L_β} are aerodynamic lift derivatives due to the angle of attack and the deflection of trailing-edge control surface; and C_{M_α} and C_{M_β} are the aerodynamic moment derivatives.

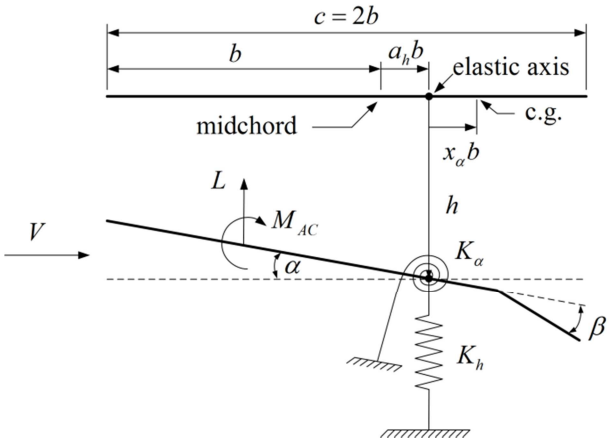

Fig. 1 The aeroelastic model with pitch and plunge degrees of freedom

In this paper, bounded nonlinear torsional uncertainty and control input disturbance are considered. Then by combining equations (1)-(4) and introducing the nonlinear uncertainty and input disturbance, it is found that,

$$\mathbf{A}\ddot{\mathbf{q}} + (\mathbf{D}+\mathbf{B})\dot{\mathbf{q}} + (\mathbf{C}+\mathbf{E})\mathbf{q} + \Delta\mathbf{E}\mathbf{q} = \mathbf{b}(\beta + \Delta\beta) \tag{5}$$

where,

$$\mathbf{A}=\begin{bmatrix} m_T & m_W x_\alpha b \\ m_W x_\alpha b & I_\alpha \end{bmatrix},\ \mathbf{B}=\begin{bmatrix} \rho V b s_W C_{L_\alpha} & \rho V b^2 s_W C_{L_\alpha}\left(1/2-a_h\right) \\ -\rho V b^2 s_W C_{M_\alpha} & -\rho V b^3 s_W C_{M_\alpha}\left(1/2-a_h\right) \end{bmatrix},\ \mathbf{b}=\begin{pmatrix} -\rho V^2 b s_W C_{L_\beta} \\ \rho V^2 b^2 s_W C_{M_\beta} \end{pmatrix}$$

$$\mathbf{C}=\begin{bmatrix} 0 & \rho V^2 b s_W C_{L_\alpha} \\ 0 & -\rho V^2 b^2 s_W C_{M_\alpha} \end{bmatrix},\mathbf{D}=\begin{bmatrix} C_h & 0 \\ 0 & C_\alpha \end{bmatrix},\ \mathbf{E}=\begin{bmatrix} K_h & 0 \\ 0 & K_\alpha(\alpha) \end{bmatrix},\ \Delta\mathbf{E}=\begin{bmatrix} 0 & 0 \\ 0 & \Delta K_\alpha(\alpha) \end{bmatrix},\ \mathbf{q}=\begin{pmatrix} h \\ \alpha \end{pmatrix}.$$

and $\Delta K_\alpha(\alpha)$ and $\Delta\beta$ represent the nonlinear torsional uncertainty and input disturbance respectively.

It is assumed that the structural nonlinearity uncertainty is bounded by,

$$\left|\Delta K_\alpha(\alpha)\alpha\right| \le \left|n(\alpha)\alpha\right| \tag{6}$$

where $n(\alpha)$ is a known upper bound of the uncertain nonlinearity.

If $\begin{bmatrix} h & \alpha & \dot{h} & \dot{\alpha} \end{bmatrix}^T = \begin{bmatrix} x_1 & x_2 & x_3 & x_4 \end{bmatrix}^T = \mathbf{x}^T$, then Equations in (5) may be cast in state-space form,

$$\dot{\mathbf{x}} = \mathbf{f}(\mathbf{x}) + \mathbf{g}(\beta + \Delta\beta) + \boldsymbol{\delta} \tag{7}$$

where,

$$\mathbf{f}(\mathbf{x})=\begin{pmatrix} x_3 \\ x_4 \\ -k_1 x_1 - \left(k_2 V^2 + p(x_2)\right)x_2 - c_1 x_3 - c_2 x_4 \\ -k_3 x_1 - \left(k_4 V^2 + q(x_2)\right)x_2 - c_3 x_3 - c_4 x_4 \end{pmatrix},\ \mathbf{g}=\begin{pmatrix} 0 \\ 0 \\ g_3 \\ g_4 \end{pmatrix},\ \boldsymbol{\delta}=\mathbf{t}\Delta K_\alpha(x_2)x_2,\ \mathbf{t}=\begin{pmatrix} 0 \\ 0 \\ t_3 \\ t_4 \end{pmatrix},$$

$$d = m_T I_\alpha - m_W^2 x_\alpha^2 b^2,\ k_1 = I_\alpha K_h/d,\ k_2 = \left(I_\alpha \rho b s_W C_{L_\alpha} + m_W x_\alpha \rho b^3 s_W C_{M_\alpha}\right)/d,$$

$$k_3 = -m_W x_\alpha b K_h/d,\ k_4 = -\left(m_W x_\alpha \rho b^2 s_W C_{L_\alpha} + m_T \rho b^2 s_W C_{M_\alpha}\right)/d,$$

$$p(x_2) = -m_W x_\alpha b K_\alpha(x_2)/d,\ c_1 = \left[I_\alpha\left(C_h + \rho V b s_W C_{L_\alpha}\right) + m_W x_\alpha \rho V b^3 s_W C_{M_\alpha}\right]/d,$$

$$q(x_2) = m_T K_\alpha(x_2)/d,\ c_3 = \left[-m_W x_\alpha b\left(C_h + \rho V b s_W C_{L_\alpha}\right) - m_T \rho V b^2 s_W C_{M_\alpha}\right]/d,$$

$$c_2 = \left[I_\alpha \rho V b^2 s_W C_{L_\alpha}\left(1/2-a_h\right) - m_W x_\alpha b C_\alpha + m_W x_\alpha \rho V b^4 s_W C_{M_\alpha}\left(1/2-a_h\right)\right]/d,$$

$$c_4 = \left[m_T\left(C_\alpha - \rho V b^3 s_W C_{M_\alpha}\left(1/2-a_h\right)\right) - m_W x_\alpha \rho V b^3 s_W C_{L_\alpha}\left(1/2-a_h\right)\right]/d,$$

$$g_3 = -V^2\left(I_\alpha \rho b s_W C_{L_\beta} + m_W x_\alpha \rho b^3 s_W C_{M_\beta}\right)\Big/ d\ ,\ g_4 = V^2\left(m_W x_\alpha \rho b^2 s_W C_{L_\beta} + m_T \rho b^2 s_W C_{M_\beta}\right)\Big/ d\ ,$$

$$t_3 = m_W x_\alpha b/d \ \text{ and } \ t_4 = -m_T/d$$

3. Normal Form

In this paper, the pitch angle is selected as the output feedback variable,

$$y = x_2 = \alpha \tag{8}$$

The relative degree of the system, denoted by r, is determined by the number of times the output can be differentiated until the input appears explicitly in the expression for the r^{th} time derivative. In the present case,

$$\begin{aligned}
&y = x_2 \\
&\dot{y} = \frac{\mathrm{d}y}{\mathrm{d}\mathbf{x}}.\frac{\mathrm{d}\mathbf{x}}{\mathrm{d}t} = \frac{\mathrm{d}y}{\mathrm{d}\mathbf{x}}\cdot\left(\mathbf{f}\left(\mathbf{x}\right)+\mathbf{g}\cdot\left(\beta+\Delta\beta\right)+\boldsymbol{\delta}\right) \\
&\quad = \begin{bmatrix}0 & 1 & 0 & 0\end{bmatrix}\begin{pmatrix} x_3 \\ x_4 \\ -k_1x_1-\left(k_2V^2+p\left(x_2\right)\right)x_2-c_1x_3-c_2x_4+g_3\left(\beta+\Delta\beta\right)+t_3\Delta K_\alpha\left(x_2\right)x_2 \\ -k_3x_1-\left(k_4V^2+q\left(x_2\right)\right)x_2-c_3x_3-c_4x_4+g_4\left(\beta+\Delta\beta\right)+t_4\Delta K_\alpha\left(x_2\right)x_2 \end{pmatrix} = x_4 \\
&\ddot{y} = \frac{\mathrm{d}\dot{y}}{\mathrm{d}\mathbf{x}}.\frac{\mathrm{d}\mathbf{x}}{\mathrm{d}t} = \frac{\mathrm{d}x_4}{\mathrm{d}\mathbf{x}}\cdot\left(\mathbf{f}\left(\mathbf{x}\right)+\mathbf{g}\cdot\left(\beta+\Delta\beta\right)+\boldsymbol{\delta}\right) \\
&\quad = \begin{bmatrix}0 & 0 & 0 & 1\end{bmatrix}\cdot\left(\mathbf{f}\left(\mathbf{x}\right)+\mathbf{g}\cdot\left(\beta+\Delta\beta\right)+\boldsymbol{\delta}\right) \\
&\quad = -k_3x_1-\left(k_4V^2+q\left(x_2\right)\right)x_2-c_3x_3-c_4x_4+g_4\left(\beta+\Delta\beta\right)+\delta_2
\end{aligned} \tag{9}$$

where $\delta_2 = t_4\Delta K_\alpha\left(x_2\right)x_2$.

Since the input $g_4\left(\beta+\Delta\beta\right)$ appears in the expression for $\ddot{y}$ it is apparent that relative degree $r=2$. The significance of this is that the nonlinear system may be divided into an external sub-system of dimension r, generally with nonlinear input, and a sub-system of $n-r$ nonlinear equations known as the internal dynamics. In the present case both subsystems are of order 2. This arrangement of equations is known as the normal form, which in the present case may be obtained by means of the transformation,

$$\mathbf{z} = \mathbf{T}\mathbf{x} \ \text{ or } \ \begin{pmatrix} z_1 \\ z_2 \\ z_3 \\ z_4 \end{pmatrix} = \begin{bmatrix} -g_4 & g_3 & 0 & 0 \\ 0 & 1 & g_4/\varphi_4 & -g_3/\varphi_4 \\ 0 & 1 & 0 & 0 \\ 0 & 0 & 0 & 1 \end{bmatrix}\begin{pmatrix} x_1 \\ x_2 \\ x_3 \\ x_4 \end{pmatrix} \tag{10}$$

where $\varphi_4 = g_3 c_1 + g_4 c_2 - c_3 g_3^2 / g_4 - c_4 g_3$, such that $\frac{dz_1}{d\mathbf{x}}\mathbf{g} = 0$, $\frac{dz_2}{d\mathbf{x}}\mathbf{g} = 0$ to ensure that the input does not appear explicitly in the equations of the internal dynamics. The matrix $\mathbf{T}$, being invertible, is a global diffeomorphism.

Application of equation (10), in (7) leads to the normal form,

$$\dot{\mathbf{z}}_{(1-2)} = \mathbf{f}_1\left(\mathbf{z}_{(1-2)}\right) + \mathbf{f}_2\left(\mathbf{z}_{(1-2)}, z_3\right) z_3 + \boldsymbol{\delta}_1 \tag{11}$$

$$\dot{z}_3 = z_4 \tag{12}$$

$$\dot{z}_4 = f_b\left(\mathbf{z}\right) + g_4 \cdot \left(\beta + \Delta\beta\right) + \delta_2 \tag{13}$$

where,

$$\mathbf{f}_1\left(\mathbf{z}_{(1-2)}\right) = \mathbf{S}\mathbf{z}_{(1-2)} = \begin{bmatrix} 0 & -\varphi_4 \\ -\varphi_1/\varphi_4 & \varphi_2 \end{bmatrix} \mathbf{z}_{(1-2)} \tag{14}$$

$$\mathbf{f}_2\left(\mathbf{z}_{(1-2)}, z_3\right) = \begin{pmatrix} \varphi_4 \\ \left(-\frac{1}{\varphi_4}\right)\left(\varphi_2\varphi_4 + \varphi_{31} + \varphi_{32} K_\alpha\left(z_3\right)\right) \end{pmatrix} \tag{15}$$

$$f_b\left(\mathbf{z}\right) = \varphi_7 z_1 + \varphi_4\varphi_8\left(z_3 - z_2\right) + \varphi_{91} z_3 + \varphi_{92} K_\alpha\left(z_3\right) z_3 + \varphi_{10} z_4 \tag{16}$$

$$\mathbf{z}_{(1-2)} = \begin{pmatrix} z_1 \\ z_2 \end{pmatrix},\ \boldsymbol{\delta}_1 = \tilde{\mathbf{t}}\Delta K_\alpha\left(z_3\right) z_3,\ \tilde{\mathbf{t}} = \begin{pmatrix} 0 \\ \tilde{t}_2 \end{pmatrix} = \begin{pmatrix} 0 \\ \dfrac{g_4 m_W x_\alpha b + g_3 m_T}{\varphi_4 d} \end{pmatrix} \tag{17}$$

$$\varphi_1 = k_3\left(g_3/g_4\right) - k_1,\ \varphi_{31} = g_3 k_1 + g_4 k_2 V^2 - k_3\left(g_3^2/g_4\right) - g_3 k_4 V^2 \tag{18}$$

$$\varphi_2 = c_3\left(g_3/g_4\right) - c_1,\ \varphi_{32} = -\left(g_4 m_W x_\alpha b + g_3 m_T\right)/d,\ \varphi_7 = k_3/g_4,\ \varphi_8 = c_3/g_4 \tag{19}$$

$$\varphi_{91} = -\left(k_3\left(g_3/g_4\right) + k_4 V^2\right),\ \varphi_{92} = -m_T/d \text{ and } \varphi_{10} = -\left(c_3\left(g_3/g_4\right) + c_4\right) \tag{20}$$

In the new coordinate system, equations (12) and (13) comprise a chain of simple integrators whereas the internal dynamics, determined by equation (11), are not directly affected by the control input. Together, equations (11)-(13) define a cascaded system of equations in the normal form. The structural nonlinearity uncertainty is represented in the new coordinate system in the form of unmatched and matched uncertainties $\boldsymbol{\delta}_1 \neq \mathbf{0}$ and $\delta_2 \neq 0$.

The zero dynamics of the system (11)-(13), without uncertainty and disturbance, are given by the linear system,

$$\dot{\mathbf{z}}_{(1-2)} = \mathbf{f}_1\left(\mathbf{z}_{(1-2)}\right) = \mathbf{S}\mathbf{z}_{(1-2)} \tag{21}$$

when the output is set to zero, $y = z_3 = 0$, which in turn causes z_4 to vanish, i.e. $z_4 = 0$. The zero dynamics in nonlinear systems is equivalent to the zero dynamics in LTI systems in that stability of the zero dynamics means that the system is minimum phase. In feedback linearisation, the global exponential stability of the zero dynamics is a necessary condition for the global asymptotic stability of the overall system, the sufficient condition being that the internal dynamics is input-to-state stable [28]. The nonlinear system is globally minimum phase if the zero dynamics has a global, asymptotically-stable equilibrium point. It is apparent from equation (21) that in the present case the zero-dynamics system is nominal even in the presence of pitch stiffness uncertainty.

In this paper, we will employ sliding-mode control to stabilise the nonlinear system (11)-(13). The idea of sliding-mode control is to design a control input β to force the system states to move toward a desired stable sliding surface, $s = 0$, and maintain the states on it. Once on the sliding surface, all the states will move along the sliding surface and converge to zero. On the sliding surface, the behaviour of the system is determined by the prescribed sliding surface. It will be shown later that the design of a stable sliding-mode surface will stabilise the internal dynamics.

Due to the form of equations (11)-(13) it is convenient to choose a nonlinear sliding surface as,

$$s = z_4 - \Phi_1\left(\mathbf{z}_{(1-3)}\right) = 0 \tag{22}$$

where $\mathbf{z}_{(1-3)} = \left[\mathbf{z}_{(1-2)}^T, z_3\right]^T$ and $\Phi_1\left(\mathbf{z}_{(1-3)}\right)$ is an unknown function to be designed with the requirement that the origin of the dynamics of the reduced-order model,

$$\dot{\mathbf{z}}_{(1-2)} = \mathbf{f}_1\left(\mathbf{z}_{(1-2)}\right) + \mathbf{f}_2\left(\mathbf{z}_{(1-2)}, z_3\right) z_3 + \boldsymbol{\delta}_1 \tag{23}$$

$$\dot{z}_3 = \Phi_1\left(\mathbf{z}_{(1-3)}\right) \tag{24}$$

confined to the sliding surface, shall be globally asymptotically stable. The design of $\Phi_1\left(\mathbf{z}_{(1-3)}\right)$ amounts to solving a stabilisation problem for the system (23)-(24) with $z_4 = \Phi_1\left(\mathbf{z}_{(1-3)}\right)$ viewed as the control input.

In view of its importance, the stability properties of the zero dynamics of system (11)-(13) will now be considered. Suppose the origin of zero dynamics $\dot{\mathbf{z}}_{(1-2)} = \mathbf{f}_1\left(\mathbf{z}_{(1-2)}\right) = \mathbf{S}\mathbf{z}_{(1-2)}$ is globally asymptotically stable, then $\mathbf{S}$ is Hurwitz, $\det\left(\mathbf{S} - \lambda\mathbf{I}\right) = \lambda^2 - \varphi_2\lambda - \varphi_1$ so that $\varphi_1, \varphi_2 < 0$. Hence, for any given positive definite symmetric matrix $\mathbf{Q}$, there exists a positive definite symmetric matrix $\mathbf{P}$ that satisfies the Lyapunov equation,

$$\mathbf{PS} + \mathbf{S}^T\mathbf{P} = -\mathbf{Q} \tag{25}$$

Correspondingly, there exists a continuously differentiable, radially unbounded storage function[1] $W(\mathbf{z})$ satisfying,

$$\lambda_{\min}(\mathbf{P})\left\|\mathbf{z}_{(1-2)}\right\|_2^2 \le W\left(\mathbf{z}_{(1-2)}\right) = \mathbf{z}_{(1-2)}^T\mathbf{P}\mathbf{z}_{(1-2)} \le \lambda_{\max}(\mathbf{P})\left\|\mathbf{z}_{(1-2)}\right\|_2^2 \tag{26}$$

and,

$$\dot{W}\left(\mathbf{z}_{(1-2)}\right) = \frac{\mathrm{d}W\left(\mathbf{z}_{(1-2)}\right)}{\mathrm{d}\mathbf{z}_{(1-2)}}\mathbf{f}_1\left(\mathbf{z}_{(1-2)}\right) = -\mathbf{z}_{(1-2)}{}^T\mathbf{Q}\mathbf{z}_{(1-2)} \le -\lambda_{\min}(\mathbf{Q})\left\|\mathbf{z}_{(1-2)}\right\|_2^2 \tag{27}$$

for $\forall\mathbf{z}_{(1-2)} \in R^{2\times1}$, where $\dot{W}\left(\mathbf{z}_{(1-2)}\right)$ and $\mathrm{d}W\left(\mathbf{z}_{(1-2)}\right)/\mathrm{d}\mathbf{z}_{(1-2)}$ are the differentials of $W\left(\mathbf{z}_{(1-2)}\right)$ with respect to time t and $\mathbf{z}_{(1-2)}$ respectively, $\lambda_{\min}(\bullet)$ and $\lambda_{\max}(\bullet)$ are minimum and maximum eigenvalues of $(\bullet)$, and $\left\|(\bullet)\right\|_2$ is the Euclidean norm of $(\bullet)$ [28].

In the analysis above, positive-definite $\mathbf{Q}$ may be chosen arbitrarily, but in this paper is taken to be,

$$\mathbf{Q} = \begin{bmatrix} q_1 & 0 \\ 0 & q_2 \end{bmatrix},\ q_1 > 0,\ q_2 > 0 \tag{28}$$

Then $\mathbf{P}$ is found as,

$$\mathbf{P} = \begin{bmatrix} p_{11} & p_{12} \\ p_{12} & p_{22} \end{bmatrix} = \begin{bmatrix} \dfrac{\varphi_1 q_2}{2\varphi_2\varphi_4^2} - \dfrac{q_1}{2\varphi_2} + \dfrac{\varphi_2 q_1}{2\varphi_1} & \dfrac{\varphi_4 q_1}{2\varphi_1} \\ \dfrac{\varphi_4 q_1}{2\varphi_1} & -\dfrac{q_2}{2\varphi_2} + \dfrac{\varphi_4^2 q_1}{2\varphi_1\varphi_2} \end{bmatrix} \tag{29}$$

which is indeed a positive-definite, symmetric matrix. Since the zero dynamics are linear they are not only globally asymptotically stable but converge to zero exponentially.

4. Robust passivity-based continuous sliding mode controller design

This section presents the design of a sliding mode controller. Firstly, a robust stable sliding-mode surface $s = 0$ is designed such that the internal dynamics is stabilised. Then, a control input β is designed to force the system states to move toward the designed stable sliding surface $s = 0$ and maintain the states on it. Once on the sliding surface, all the states will move along the sliding surface and converge to zero.

[1] A radially unbounded function is a function $W(\mathbf{z})$ for which $\|\mathbf{z}\| \to \infty \Rightarrow W(\mathbf{z}) \to \infty$.

4.1. Robust passivity-based sliding surface design

Consider the system (11) and (12). z_4 may be viewed as the input to the system and z_3 the output variable. According to the definition of robust passivity [30], and using equations (11) and (12), the system (11), (12) is said to be robust strictly passive if there exists a differentiable and positive definite storage function $U_1\left(\mathbf{z}_{(1-3)}\right)$ such that,

$$\dot{U}_1 = \frac{dU_1\left(\mathbf{z}_{(1-3)}\right)}{d\mathbf{z}_{(1-3)}}\begin{pmatrix}\mathbf{f}_1\left(\mathbf{z}_{(1-2)}\right)+\mathbf{f}_2\left(\mathbf{z}_{(1-2)}, z_3\right)z_3+\boldsymbol{\delta}_1\\ z_4\end{pmatrix} < z_3 z_4,\ \ \forall z_3 \neq 0 \tag{30}$$

holds for any $\boldsymbol{\delta}_1$ subjected to the constraint (6). This may be understood physically as follows. If $U_1\left(\mathbf{z}_{(1-3)}\right)$ represents the energy of the system, then inequality (30) indicates that the system (11) and (12) is dissipative because the energy storage rate is less than the external energy supply rate $z_3 z_4$, with the difference being the energy dissipation rate. If z_4 is designed such that $\dot{U}_1 < 0$ with $\forall z_3 \neq 0$, then the system can be stabilised with input z_4. Here, the robust feedback passivity property [28, 31] is used to design $z_4 = \Phi_1\left(\mathbf{z}_{(1-3)}\right)$ such that global stability of the system (11) and (12) is obtained.

Lemma 4.1 Suppose the origin of the zero dynamics $\dot{\mathbf{z}}_{(1-2)} = \mathbf{f}_1\left(\mathbf{z}_{(1-2)}\right) = \mathbf{S}\mathbf{z}_{(1-2)}$ is globally exponentially stable and let $W\left(\mathbf{z}_{(1-2)}\right)$ be a continuously differentiable, radially unbounded Lyapunov function candidate satisfying (26) and (27). Then there exists a positive real constant λ such that,

$$\frac{dW\left(\mathbf{z}_{(1-2)}\right)}{d\mathbf{z}_{(1-2)}}\mathbf{f}_1 + \frac{\lambda}{2}\left(\frac{dW\left(\mathbf{z}_{(1-2)}\right)}{d\mathbf{z}_{(1-2)}}\tilde{\mathbf{t}}\right)^2 < -\gamma_1\left\|\mathbf{z}_{(1-2)}\right\|_2^2 \tag{31}$$

where γ_1 is a positive constant.

Proof: Since $\dot{\mathbf{z}}_{(1-2)} = \mathbf{f}_1\left(\mathbf{z}_{(1-2)}\right) = \mathbf{S}\mathbf{z}_{(1-2)}$ is globally exponentially stable, there exists a continuously differentiable, radially unbounded Lyapunov function $W\left(\mathbf{z}_{(1-2)}\right)$ satisfying (26) and (27). Thus from (26),

$$\frac{dW\left(\mathbf{z}_{(1-2)}\right)}{d\mathbf{z}_{(1-2)}}\tilde{\mathbf{t}} = 2\mathbf{z}_{(1-2)}^T\mathbf{P}\tilde{\mathbf{t}} = 2\tilde{t}_2\left(z_1 p_{12} + z_2 p_{22}\right) \tag{32}$$

Therefore,

$$\begin{aligned}&\frac{dW\left(\mathbf{z}_{(1-2)}\right)}{d\mathbf{z}_{(1-2)}}\mathbf{f}_1+\frac{\lambda}{2}\left(\frac{dW\left(\mathbf{z}_{(1-2)}\right)}{d\mathbf{z}_{(1-2)}}\tilde{\mathbf{t}}\right)^2\\&=\frac{dW\left(\mathbf{z}_{(1-2)}\right)}{d\mathbf{z}_{(1-2)}}\mathbf{f}_1+2\lambda\tilde{t}_2^2\left(z_1p_{12}+z_2p_{22}\right)^2\end{aligned}\tag{33}$$

Then, due to (27) and the expression,

$$\left(z_1p_{12}+z_2p_{22}\right)^2\le 2\left(z_1p_{12}\right)^2+2\left(z_2p_{22}\right)^2\le 2\max\left(p_{12}^2,p_{22}^2\right)\left(z_1^2+z_2^2\right)\tag{34}$$

equation (33) becomes,

$$\begin{aligned}&\frac{dW\left(\mathbf{z}_{(1-2)}\right)}{d\mathbf{z}_{(1-2)}}\mathbf{f}_1+\frac{\lambda}{2}\left(\frac{dW\left(\mathbf{z}_{(1-2)}\right)}{d\mathbf{z}_{(1-2)}}\tilde{\mathbf{t}}\right)^2\\&\le-\left[\lambda_{\min}\left(\mathbf{Q}\right)-4\lambda\tilde{t}_2^2\max\left(p_{12}^2,p_{22}^2\right)\right]\left\|\mathbf{z}_{(1-2)}\right\|_2^2\\&=-\gamma_1\left\|\mathbf{z}_{(1-2)}\right\|_2^2\end{aligned}\tag{35}$$

where $\gamma_1>0$ provided that $\lambda<\dfrac{\lambda_{\min}\left(\mathbf{Q}\right)}{4\tilde{t}_2^2\max\left(p_{12}^2,p_{22}^2\right)}$.

□

Lemma 4.2 Suppose the origin of the zero dynamics $\dot{\mathbf{z}}_{(1-2)}=\mathbf{f}_1\left(\mathbf{z}_{(1-2)}\right)=\mathbf{S}\mathbf{z}_{(1-2)}$ is globally exponentially stable, then the origin of the uncertain subsystem (11)-(12) can be globally exponentially stabilised by,

$$z_4=\Phi_1\left(\mathbf{z}_{(1-3)}\right)=-\frac{dW\left(\mathbf{z}_{(1-2)}\right)}{d\mathbf{z}_{(1-2)}}\mathbf{f}_2-\frac{1}{2\lambda}n^2\left(z_3\right)z_3-\chi z_3\tag{36}$$

where $W\left(\mathbf{z}_{(1-2)}\right)$ is a radially unbounded, positive-definite Lyapunov function satisfying (26) and (27).

Proof: Suppose the origin of the zero dynamics $\dot{\mathbf{z}}_{(1-2)}=\mathbf{f}_1\left(\mathbf{z}_{(1-2)}\right)=\mathbf{S}\mathbf{z}_{(1-2)}$ is globally exponentially stable and there exist a radially unbounded, positive definite Lyapunov function $W\left(\mathbf{z}_{(1-2)}\right)$ satisfying (26) and (27).

Take a storage function candidate,

$$U_1\left(\mathbf{z}_{(1-3)}\right)=W\left(\mathbf{z}_{(1-2)}\right)+\frac{1}{2}z_3^2 \tag{37}$$

for the uncertain subsystem (11)-(12), where $W\left(\mathbf{z}_{(1-2)}\right)$ satisfies (26) and (27). It may be shown that,

$$\min\left(\lambda_{\min}\left(\mathbf{P}\right),\frac{1}{2}\right)\left\|\mathbf{z}_{(1-3)}\right\|_2^2\le U_1\left(\mathbf{z}_{(1-3)}\right)\le\max\left(\lambda_{\max}\left(\mathbf{P}\right),\frac{1}{2}\right)\left\|\mathbf{z}_{(1-3)}\right\|_2^2 \tag{38}$$

The derivate of U_1 is,

$$\dot{U}_1=\frac{\mathrm{d}U_1}{\mathrm{d}\mathbf{z}_{(1-3)}}\dot{\mathbf{z}}_{(1-3)}=\begin{bmatrix}\dfrac{\mathrm{d}W\left(\mathbf{z}_{(1-2)}\right)}{\mathrm{d}\mathbf{z}_{(1-2)}} & z_3\end{bmatrix}\begin{bmatrix}\dot{\mathbf{z}}_{(1-2)}\\ \dot{z}_3\end{bmatrix} \tag{39}$$

Substitution of (11) and (12) in (39) leads to,

$$\begin{aligned}\dot{U}_1&=\frac{dW\left(\mathbf{z}_{(1-2)}\right)}{d\mathbf{z}_{(1-2)}}\mathbf{f}_1+z_3\frac{dW\left(\mathbf{z}_{(1-2)}\right)}{d\mathbf{z}_{(1-2)}}\mathbf{f}_2+\frac{dW\left(\mathbf{z}_{(1-2)}\right)}{d\mathbf{z}_{(1-2)}}\boldsymbol{\delta}_1+z_3z_4\\&\le\frac{dW\left(\mathbf{z}_{(1-2)}\right)}{d\mathbf{z}_{(1-2)}}\mathbf{f}_1+z_3\frac{dW\left(\mathbf{z}_{(1-2)}\right)}{d\mathbf{z}_{(1-2)}}\mathbf{f}_2+z_3z_4+\left|\frac{dW\left(\mathbf{z}_{(1-2)}\right)}{d\mathbf{z}_{(1-2)}}\tilde{\mathbf{t}}\right|\left|\Delta K_\alpha\left(z_3\right)z_3\right|\end{aligned} \tag{40}$$

and using the bound on the nonlinearity (6),

$$\dot{U}_1\le\frac{dW\left(\mathbf{z}_{(1-2)}\right)}{d\mathbf{z}_{(1-2)}}\mathbf{f}_1+z_3\frac{dW\left(\mathbf{z}_{(1-2)}\right)}{d\mathbf{z}_{(1-2)}}\mathbf{f}_2+z_3z_4+\left|\frac{dW\left(\mathbf{z}_{(1-2)}\right)}{d\mathbf{z}_{(1-2)}}\tilde{\mathbf{t}}\right|\left|n\left(z_3\right)z_3\right| \tag{41}$$

Since,

$$\begin{aligned}\left|\frac{dW\left(\mathbf{z}_{(1-2)}\right)}{d\mathbf{z}_{(1-2)}}\tilde{\mathbf{t}}\right|\left|n\left(z_3\right)z_3\right|&=\left(\left|\frac{dW\left(\mathbf{z}_{(1-2)}\right)}{d\mathbf{z}_{(1-2)}}\tilde{\mathbf{t}}\right|\sqrt{\lambda}\right)\left(\frac{1}{\sqrt{\lambda}}\left|n\left(z_3\right)z_3\right|\right)\\&\le\frac{1}{2}\left(\left|\frac{dW\left(\mathbf{z}_{(1-2)}\right)}{d\mathbf{z}_{(1-2)}}\tilde{\mathbf{t}}\right|\sqrt{\lambda}\right)^2+\frac{1}{2}\left(\frac{1}{\sqrt{\lambda}}\left|n\left(z_3\right)z_3\right|\right)^2\\&=\frac{\lambda}{2}\left(\frac{dW\left(\mathbf{z}_{(1-2)}\right)}{d\mathbf{z}_{(1-2)}}\tilde{\mathbf{t}}\right)^2+\frac{1}{2\lambda}n^2\left(z_3\right)z_3^2\end{aligned} \tag{42}$$

inequality (41) becomes,

$$\dot{U}_1 \le \frac{dW\left(\mathbf{z}_{(1-2)}\right)}{d\mathbf{z}_{(1-2)}}\mathbf{f}_1 + z_3\frac{dW\left(\mathbf{z}_{(1-2)}\right)}{d\mathbf{z}_{(1-2)}}\mathbf{f}_2 + z_3 z_4 + \frac{\lambda}{2}\left(\frac{dW\left(\mathbf{z}_{(1-2)}\right)}{d\mathbf{z}_{(1-2)}}\tilde{\mathbf{t}}\right)^2 + \frac{1}{2\lambda}n^2\left(z_3\right)z_3^2 \qquad (43)$$

Then, by using feedback control (36),

$$\begin{aligned}\dot{U}_1 &\le -\chi z_3^2 + \frac{dW\left(\mathbf{z}_{(1-2)}\right)}{d\mathbf{z}_{(1-2)}}\mathbf{f}_1 + \frac{\lambda}{2}\left(\frac{dW\left(\mathbf{z}_{(1-2)}\right)}{d\mathbf{z}_{(1-2)}}\tilde{\mathbf{t}}\right)^2 \\ &\le -\chi z_3^2 - \gamma_1\left\|\mathbf{z}_{(1-2)}\right\|_2^2 \\ &\le -\gamma_2\left\|\mathbf{z}_{(1-3)}\right\|_2^2\end{aligned} \qquad (44)$$

where $\gamma_2 = \min\left(\chi, \gamma_1\right) > 0$.

Hence, by invoking Theorem 4.10 [28] with inequalities (38) and (44), the origin of the system (11) and (12) is found to be globally exponentially stable.

□

Now considering the reduced order system defined by equations (11) and (12), if the zero dynamics, $\dot{\mathbf{z}}_{(1-2)} = \mathbf{f}_1\left(\mathbf{z}_{(1-2)}\right) = \mathbf{S}\mathbf{z}_{(1-2)}$, is globally exponentially stable, in the presence of bounded torsional nonlinearity uncertainty and input disturbance, the nonlinear sliding-mode surface may be chosen according to (22), repeated here as,

$$s = z_4 - \Phi_1\left(\mathbf{z}_{(1-3)}\right) = 0 \qquad (45)$$

to ensure that the reduced-order uncertain system is robustly exponentially stable. However, it is still necessary to determine the input β that ensures that the states of the system are attracted to the sliding surface and remain upon it.

4.2. Sliding mode control input design

The sliding-mode control input aims to compel the states of the system, starting away from the sliding surface $s = 0$, to move toward it (i.e., the reaching phase) and then to be maintained upon it (i.e., sliding phase). In this way the sliding surface $s = 0$ is made globally attractive. Here, an approach based on Lyapunov stability theory is used for the design of a sliding-mode control input. If a candidate Lyapunov function is selected as,

$$U_2\left(s\right) = \frac{s^2}{2} \qquad (46)$$

then the control input should be designed such that,

$$\dot{U}_2 = s\dot{s} < 0 \tag{47}$$

By differentiating equation (45) and combining this with equations (69), (11)-(12), and (14)-(17), the derivative of s may be determined as,

$$\dot{s} = \dot{z}_4 - \dot{\Phi}_1\left(\mathbf{z}_{(1-3)}\right) = \Phi_2(\mathbf{z}) + \Phi_3(\mathbf{z})\Delta K_\alpha(z_3)z_3 + g_4(\beta + \Delta\beta) \tag{48}$$

with $\Phi_2(\mathbf{z})$ given by equation (70) in Appendix 1 and,

$$\Phi_3(\mathbf{z}) = \left[t_4 + \tilde{t}_2\left(q_2 + \left(\frac{q_2}{\varphi_2\varphi_4} - \frac{\varphi_4 q_1}{\varphi_1\varphi_2}\right)\left(\varphi_{31} + \varphi_{32}K_\alpha(z_3)\right)\right)\right] \tag{49}$$

The term on the left-hand-side of inequality (47) becomes,

$$\dot{U}_2 = s\left[\Phi_2(\mathbf{z}) + \Phi_3(\mathbf{z})\Delta K_\alpha(z_3)z_3 + g_4(\beta + \Delta\beta)\right] \tag{50}$$

To ensure (47) is satisfied globally, a discontinuous sliding-mode control input may be applied in the form,

$$\beta = \left(-\frac{\Phi_2(\mathbf{z})}{g_4} - \frac{\xi(\mathbf{z}) + \xi_1}{g_4}\operatorname{sgn}(s) - \frac{\upsilon}{g_4}s\right) \tag{51}$$

where $\xi(\mathbf{z})$, ξ_1, $\upsilon > 0$. The term $-\Phi_2(\mathbf{z})/g_4$, a continuous control input, is used to neutralise the known term $\Phi_2(\mathbf{z})$ in equation (50). The other three terms in (51) have negative signs, so that deviation of the dynamic response from $s = 0$ leads to an input that returns the system to the sliding surface. Specifically, $-(\xi_1/g_4)\operatorname{sgn}(s)$ and $-(\xi(\mathbf{z})/g_4)\operatorname{sgn}(s)$ are used to compensate the input disturbance and nonlinearity uncertainty respectively. $-(\upsilon/g_4)s$ is an exponential approaching law that guarantees an exponential convergence rate in the reaching phase and consequently reduces the approaching time to the sliding surface.

Substituting (51) into (50) leads to,

$$\dot{U}_2 \le \left|\Phi_3(\mathbf{z})\right| \times \left|n(z_3)z_3\right| \times |s| - \xi(\mathbf{z})|s| + sg_4\Delta\beta - \xi_1|s| - \upsilon s^2 \tag{52}$$

It is assumed that,

$$\left|\Phi_3(\mathbf{z})\right| \times \left|n(z_3)z_3\right| \le \eta(\mathbf{z}) + \eta_0\xi(\mathbf{z}) \tag{53}$$

and,

$$\left|g_4\Delta\beta\right| \le \eta_1\xi_1 \tag{54}$$

where $\eta(\mathbf{z}) \geq 0$ is a continuous function, $0 \leq \eta_0 < 1$. η_1 and ξ_1 are chosen based upon an estimate of the input uncertainty $\Delta\beta$ and the known g_4 while $0 \leq \eta_1 < 1$.

Then by combining (52), (53) and (54) it is found that,

$$\dot{U}_2 \leq -(1-\eta_0)\xi_0|s| - (1-\eta_1)\xi_1|s| - \upsilon s^2 \leq 0 \tag{55}$$

provided that $\xi(\mathbf{z}) \geq \dfrac{\eta(\mathbf{z})}{1-\eta_0} + \xi_0$ and $\xi_0 > 0$.

Inequality (55) shows that the discontinuous control input (51) is able to compel the states of the system, with bounded torsional nonlinearity uncertainty and control input disturbance satisfying (53) and (54) respectively, to move toward the sliding surface (45). Once the states are restricted to the sliding surface (45), they exponentially converge to zero as time approaches infinity because the sliding surface (45) is designed to be globally exponentially stable. It is however well known that a discontinuous sliding control will result in chattering, which presents an obstacle to the practical application of sliding-mode control [32].

The continuous sliding-mode approach is commonly used to overcome the problem of chattering caused by the signum function in equation (51). Here, the signum function $\mathrm{sgn}(s)$ is replaced by a saturation function,

$$\mathrm{sat}\left(\frac{s}{\varepsilon}\right) = \begin{cases} \mathrm{sgn}(s) & |s| > \varepsilon \\ \dfrac{s}{\varepsilon} & |s| \leq \varepsilon \end{cases} \tag{56}$$

where ε is a small positive constant that defines a boundary layer of constant width neighbouring the sliding surface at $s = 0$.

Then the continuous sliding-mode control input becomes,

$$\beta = \left(-\frac{\Phi_2(\mathbf{z})}{g_4} - \frac{\xi(\mathbf{z}) + \xi_1}{g_4}\mathrm{sat}\left(\frac{s}{\varepsilon}\right) - \frac{\upsilon}{g_4}s \right) \tag{57}$$

If the zero dynamics are exponentially stable, the nonlinearity uncertainty is bounded by (6) and satisfies the condition (53), and the input disturbance is bounded by (54), then the system can be globally stabilised by using the continuous sliding mode control input (57) and the trajectories are shown in Appendix 2 to reach the positively invariant set,

$$\Omega_\varepsilon = \left\{ U_1\left(\mathbf{z}_{(1-3)}\right) \leq U_3(\varepsilon) \right\} \cap \left\{ |s| \leq \varepsilon \right\} \tag{58}$$

close to the sliding surface defined by a boundary layer of thickness ε and an associated energy term $U_3(\varepsilon)$ defined in the Appendix 2.

The system (11)-(12) with $z_4 = \Phi_3\left(\mathbf{z}_{(1-3)}\right)$ is globally exponentially stable. If $\eta(\mathbf{0}) = 0$, $\eta_0 = 0$ and $\Delta\beta = 0$, then for a small enough ε, the origin of the full closed-loop system is shown in Appendix 2 to be globally asymptotically stable.

Remark 1: The analysis above, and in Appendix 2, does not imply an assumption of smallness of the torsional nonlinear uncertainty and input disturbance. Hence the controller is able to admit large matched and mismatched uncertainties under the practical limitation of the control surface deflection.

Remark 2: Although in theory the continuous control input is proven to stabilise the system globally, practical limits on the control surface deflection mean that stability can only be guaranteed locally.

Remark 3: The proposed controller is also capable of stabilising the system in the presence of measurement noise, which of itself leads to a secondary input disturbance $\Delta\beta_2$ limited by the inequality(54).

Proof: Assume the control input disturbance $\Delta\beta$ consists of the primary control input disturbance $\Delta\beta_1$ and a secondary control input disturbance $\Delta\beta_2$ resulting from the measurement noise. Then we have

$$\Delta\beta = \Delta\beta_1 + \Delta\beta_2 \tag{59}$$

The discontinuous sliding mode control input synthesized from measurement noise-free state variables, described by Eq. (51), may be rewritten as

$$\beta = \left(-\frac{\Phi_2(\mathbf{z})}{g_4} - \frac{\xi(\mathbf{z}) + \xi_2 + \xi_3}{g_4} \operatorname{sgn}\left(\frac{s(\mathbf{z})}{\varepsilon} \right) - \frac{\upsilon}{g_4} s(\mathbf{z}) \right) \tag{60}$$

where $\xi_1 = \xi_2 + \xi_3$. The term $-\frac{\xi_2}{g_4}\operatorname{sgn}\left(\frac{s(\mathbf{z})}{\varepsilon}\right)$ is used for compensating $\Delta\beta_1$ and the term $-\frac{\xi_3}{g_4}\operatorname{sgn}\left(\frac{s(\mathbf{z})}{\varepsilon}\right)$ for $\Delta\beta_2$.

Denote the measurement noise as $\Delta\mathbf{z}$. Then the control input disturbance resulting from the measurement noise may be expressed as

$$\Delta\beta_2 = \beta_2 - \beta \tag{61}$$

where

$$\beta_2 = \left(-\frac{\Phi_2(\mathbf{z}+\Delta\mathbf{z})}{g_4} - \frac{\xi(\mathbf{z}+\Delta\mathbf{z}) + \xi_2 + \xi_3}{g_4} \operatorname{sgn}\left(\frac{s(\mathbf{z}+\Delta\mathbf{z})}{\varepsilon} \right) - \frac{\upsilon}{g_4} s(\mathbf{z}+\Delta\mathbf{z}) \right) \tag{62}$$

is the discontinuous sliding mode control input synthesised with noisy measured states .

In the presence of measurement noise, Eq. (47) now becomes

$$\dot{U}_2 = s\left[\Phi_2(\mathbf{z}) + \Phi_3(\mathbf{z})\Delta K_\alpha(z_3)z_3 + g_4(\beta_2 + \Delta\beta_1)\right] \tag{63}$$

and substituting Eq. (61) into Eq. (63) leads to

$$\begin{aligned}\dot{U}_2 &= s\left[\Phi_2(\mathbf{z}) + \Phi_3(\mathbf{z})\Delta K_\alpha(z_3)z_3 + g_4(\beta + \Delta\beta_2 + \Delta\beta_1)\right] \\ &= s\left[\Phi_2(\mathbf{z}) + \Phi_3(\mathbf{z})\Delta K_\alpha(z_3)z_3 + g_4(\beta + \Delta\beta)\right]\end{aligned} \tag{64}$$

which is exactly identical to Eq.(50).

Therefore, according to the analysis in the Section 4.2, when the inequality (54) holds, that is $\left|g_4(\Delta\beta_1 + \Delta\beta_2)\right| \le \eta_1(\xi_2 + \xi_3)$ or $\left|g_4\Delta\beta\right| \le \eta_1\xi_1$, the nominal control input (57) is able to stabilise the system in a noisy environment.

5. Numerical Case Study

A two-degree-of-freedom pitch-plunge prototypical wing section with torsional nonlinearity [16] is used here for the purposes of demonstration. The performance of the proposed controller is firstly investigated in the presence of nonlinear pitch-stiffness uncertainty (producing both matched and unmatched uncertain terms). Then in the second part of the case study the controller is made robust to disturbances (sinusoidal and random) added to the control input. The system parameters are given in Table 1.

Table 1 System parameters

Parameters	Value	Parameters	Value
m_T	12.3870 Kg	$C_{M\alpha}$	$(0.5+a_h)C_{L\alpha}$
m_w	2.0490 Kg	$C_{L\beta}$	3.358
b	0.135 m	$C_{M\beta}$	-1.94
ρ	1.225 Kg/m^3	K_h	2844.4 N/m
r_{cg}	$0.0873-(b+a_h b)$ m	C_h	27.43 Kg/s
I_α	$m_w r_{cg}^2 + 0.0517$ kg.m^2	C_α	0.036 Kg m^2/s
s_W	0.6 m	a_h	-0.6847
$C_{L\alpha}$	2π		

5.1. Nonlinear pitch stiffness uncertainty.

The nominal nonlinear torsional stiffness is given by,

$$K_\alpha(\alpha) = 6.8614\left(1 + 1.1438\alpha + 96.6696\alpha^2 + 9.5134\alpha^3 + 727.6641\alpha^4\right)(\text{N.m/rad}) \tag{65}$$

with globally bounded uncertainty,

$$\left\|\Delta K_\alpha(\alpha)\alpha\right\| \le 0.1\left\|K_\alpha(\alpha)\alpha\right\| \tag{66}$$

Suppose that the coefficients in (65), $k_{\alpha 1}$, $k_{\alpha 3}$ and $k_{\alpha 5}$ are 8%, 7% and 9% underestimated respectively, and $k_{\alpha 2}$ and $k_{\alpha 4}$ are 2% and 5% overestimated respectively. The nonlinear uncertainty $\Delta K_\alpha(\alpha)\alpha = 0.08k_{\alpha 1}\alpha - 0.02k_{\alpha 2}\alpha^2 + 0.07k_{\alpha 3}\alpha^3 - 0.05k_{\alpha 4}\alpha^4 + 0.09k_{\alpha 5}\alpha^5$ is found to satisfy the inequality (66).

The linear flutter boundary of the open-loop system is found to be 11.5 m/s and at velocity 16m/s, the nonlinear responses of the real system are given in Fig. 2. Clearly, the system exhibits LCO.

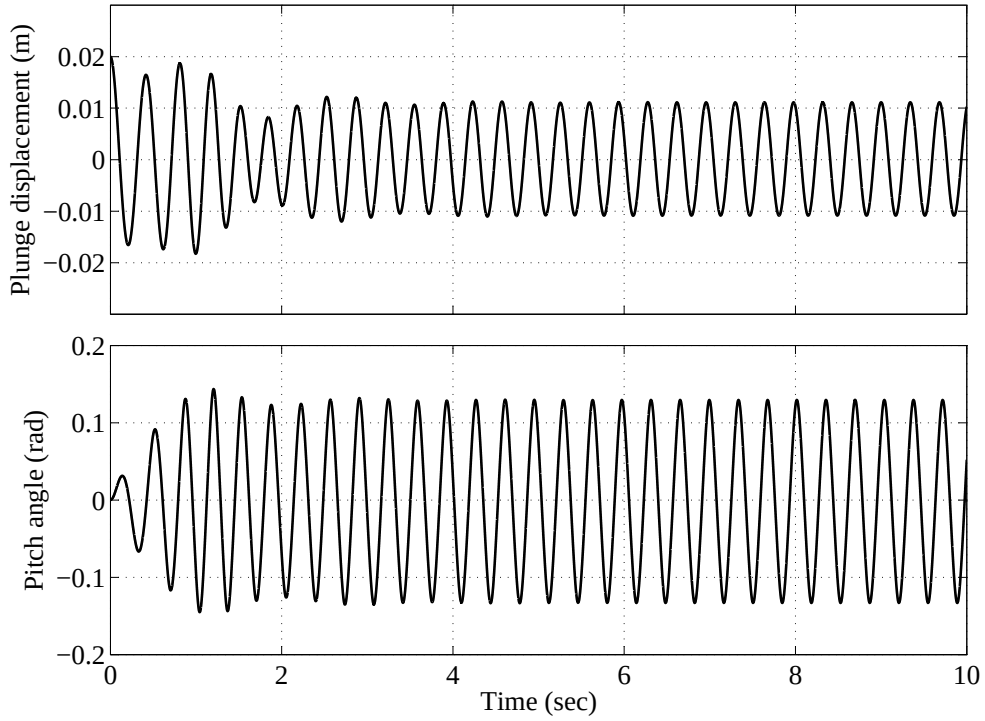

Fig. 2 The open-loop time histories with initial condition $\left[h(0) \quad \alpha(0) \quad \dot{h}(0) \quad \dot{\alpha}(0)\right]^T = [0.02 \quad 0 \quad 0 \quad 0]^T$

To demonstrate the capability of the controller in suppressing LCO at $V = 16$ m/s, the wing section is subjected to an initial disturbance, LCO becomes fully established and then the controller is activated at $t = 5$ sec.

Let,

$$\mathbf{Q} = \begin{bmatrix} 0.006 & 0 \\ 0 & 0.006 \end{bmatrix},\ \lambda = \frac{0.9\lambda_{\min}(\mathbf{Q})}{4\tilde{t}_2^2 \max\left(p_{12}^2, p_{22}^2\right)},\ \chi = 32,\quad \upsilon = 0.01,\ \xi(\mathbf{z}) = \frac{\eta(\mathbf{z})}{1-\eta_0} + \xi_0, \tag{67}$$

$$\eta_0 = 0,\ \eta_1 = 0.98,\ \xi_0 = 0.01,\ \xi_1 = 1.1,\ \varepsilon = 0.02,\ \eta(\mathbf{z}) = \left|\Phi_3(\mathbf{z})\right| \times \left|n(z_3)z_3\right|,\ \Delta\beta = 0 \tag{68}$$

The time histories with control are shown in Fig. 3, demonstrating the asymptotic stability of the closed-loop system. The matrix $\mathbf{Q}$ may be any positive definite matrix, χ and υ are arbitrarily chosen positive real numbers, λ is chosen such that $\lambda < \dfrac{\lambda_{\min}(\mathbf{Q})}{4\tilde{t}_2^2 \max\left(p_{12}^2, p_{22}^2\right)}$ and $\xi(\mathbf{z})$, ξ_0 , ξ_1 , $\eta(\mathbf{z})$, η_0 and η_1 are arbitrarily chosen such that (53), (54) and $\xi(\mathbf{z}) \geq \dfrac{\eta(\mathbf{z})}{1-\eta_0} + \xi_0$ are satisfied within the limitations of the control input level.

The sliding surface is depicted in Fig. 4, where it can be seen to begin away from the boundary layer. It firstly achieves the positively invariant set (58) and then stabilises asymptotically to the origin. This is because the origin of the reduced-order system is exponentially stable, $\eta(\mathbf{0}) = 0$ and $\eta_0 = 0$ for the current aerofoil with nonlinear pitch stiffness uncertainty and the absence of control input disturbance $\Delta\beta = 0$. The control input in Fig. 4 is seen to be smooth and within the limits of practical implementation.

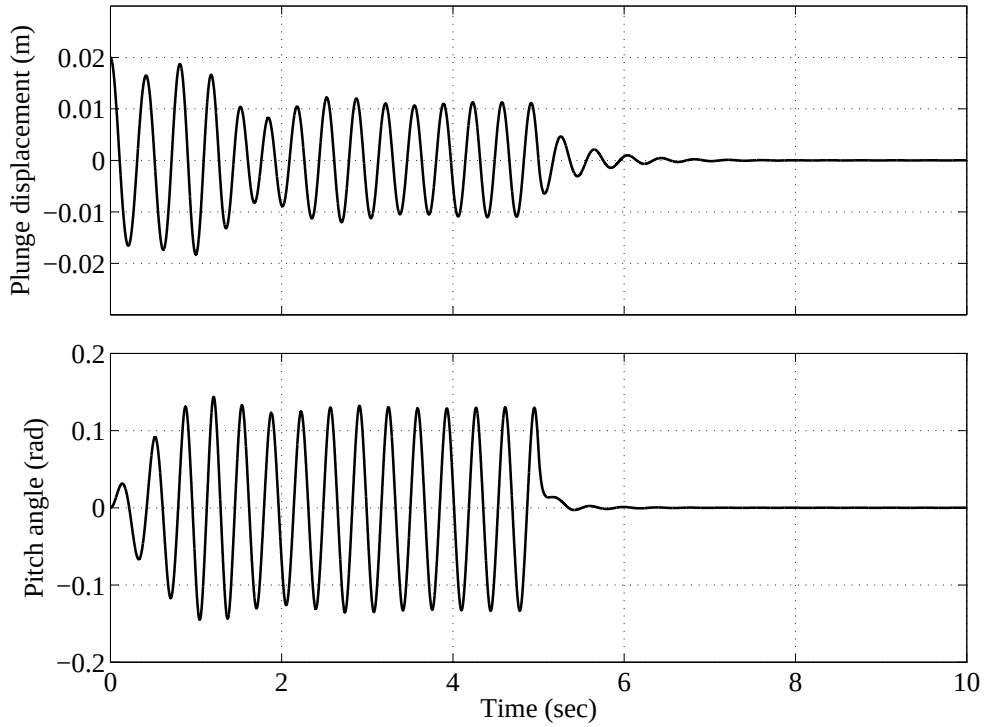

Fig. 3 Time histories of plunge displacement and pitch angle - nonlinear pitch stiffness uncertainty

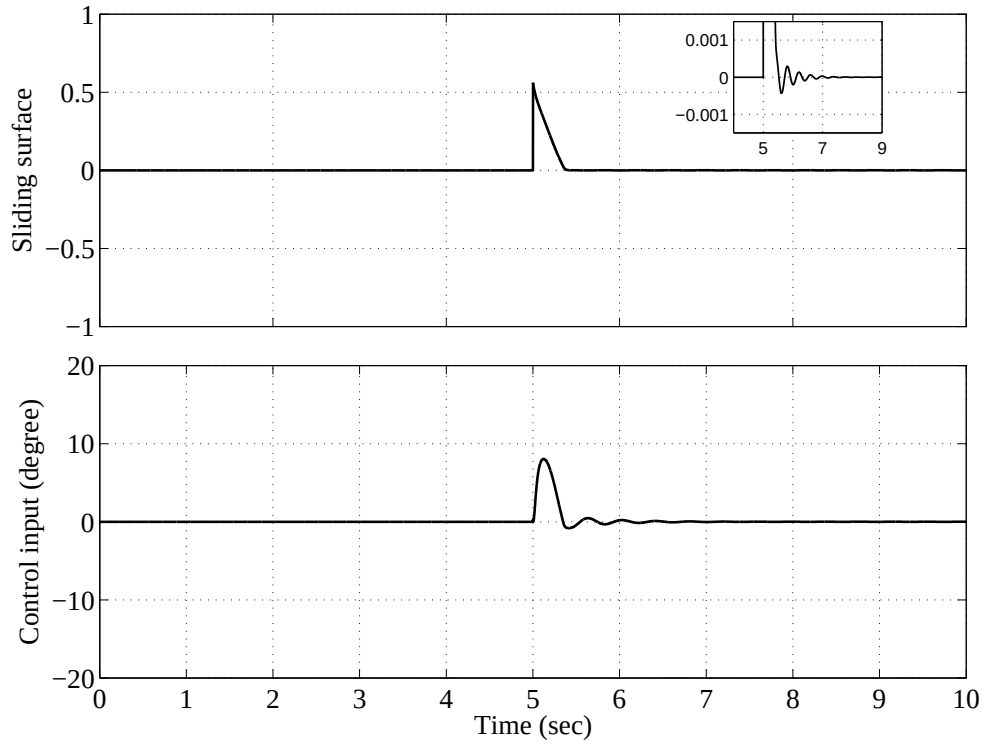

Fig. 4 Sliding surface and trailing edge control surface angle – nonlinear pitch stiffness uncertainty

5.2. Nonlinear pitch stiffness uncertainty and control input disturbance.

The robustness of the proposed controller, with parameters given in (67) and(68), to various control input disturbance, is considered. Sinusoidal and random input disturbances are chosen separately to satisfy the inequality (54). As before, the controller is activated at $t = 5\,\text{sec}$ after a LCO has been developed from an initial perturbation.

(a) Sinusoidal input disturbance.

A sinusoidal input disturbance $g_4 \Delta\beta = 0.2\sin(50t)$ is applied and time histories given in Fig. 5 show the complete state of the closed-loop system to be stable with a very low amplitude sinusoidal response. Fig. 6 confirms that the responses are bounded in a small region around the origin, as explained by (58). Also, the control input, shown in Fig. 6, is sinusoidal with low amplitude.

.

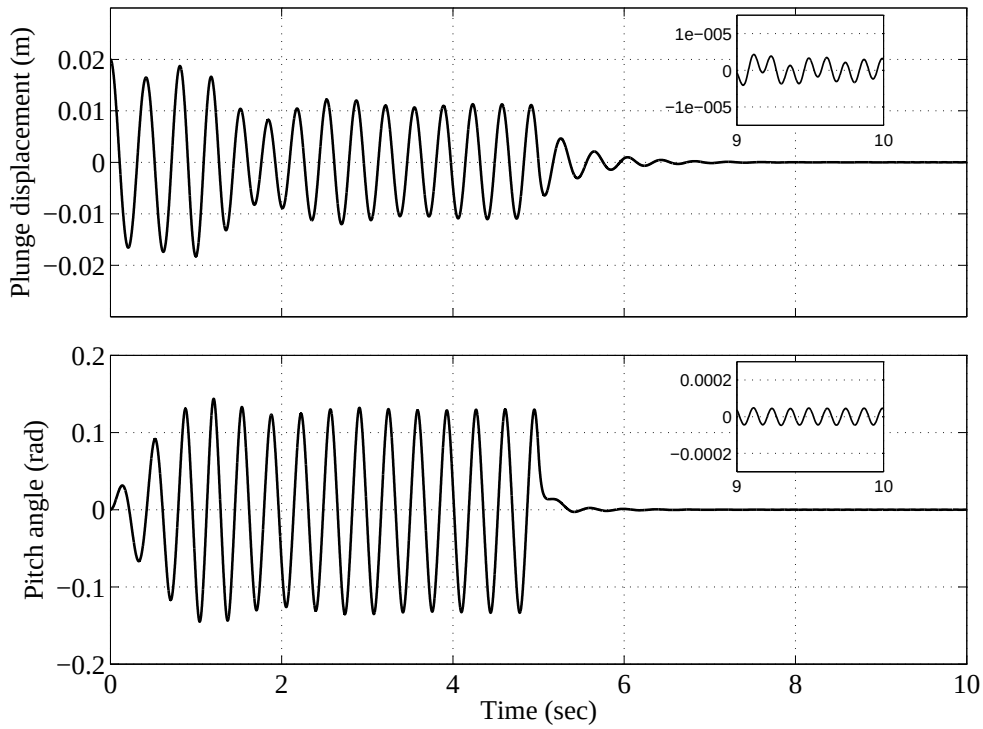

Fig. 5 Time histories of plunge displacement and pitch angle- nonlinear pitch stiffness uncertainty and sinusoidal input disturbance

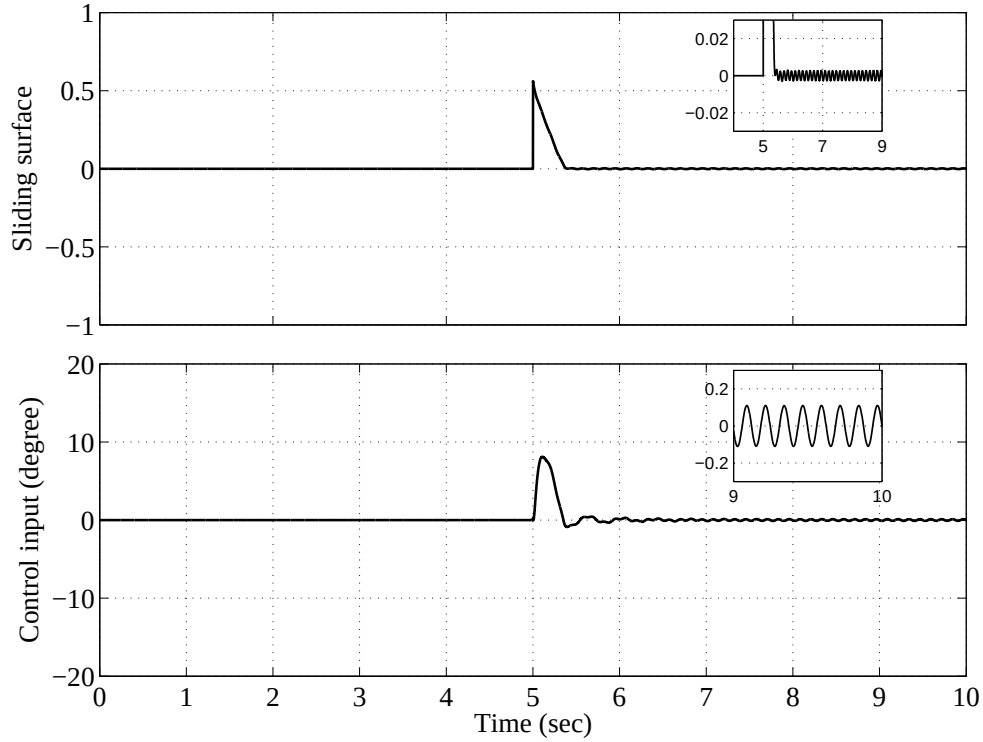

Fig. 6 Sliding surface and trailing edge control surface angle – nonlinear pitch stiffness uncertainty and sinusoidal input disturbance.

(b) Random input disturbance including the effects of measurement noise.

The measured plunge displacement, pitch angle, plunge velocity and pitch velocity are assumed to be contaminated by uniformly distributed noise of amplitude 0.0005m, 0.0002radian, 0.001m/s and 0.001radian/s respectively sampled at 0.001 second intervals. In addition, the control input disturbance $\Delta\beta_1$ is a uniformly distributed noise of amplitude 0.001 radian. The combined control input disturbance is presented in Fig. 7 where it can be seen that $\left|g_4\left(\Delta\beta_1+\Delta\beta_2\right)\right|=\left|g_4\Delta\beta\right|\le\eta_1\xi_1=1.078$. The time histories in Fig. 8 and Fig. 9 show that the complete state of the closed-loop system is stable and confined to the sliding surface with a small bounded region according to (58). The control input is seen to be random and of low amplitude.

Despite the presence of very low amplitude response – either (a) sinusoidal or (b) random - the large-amplitude open-loop responses are constrained to a very small positively invariant set around the origin, which significantly alleviates effects of nonlinear flutter.

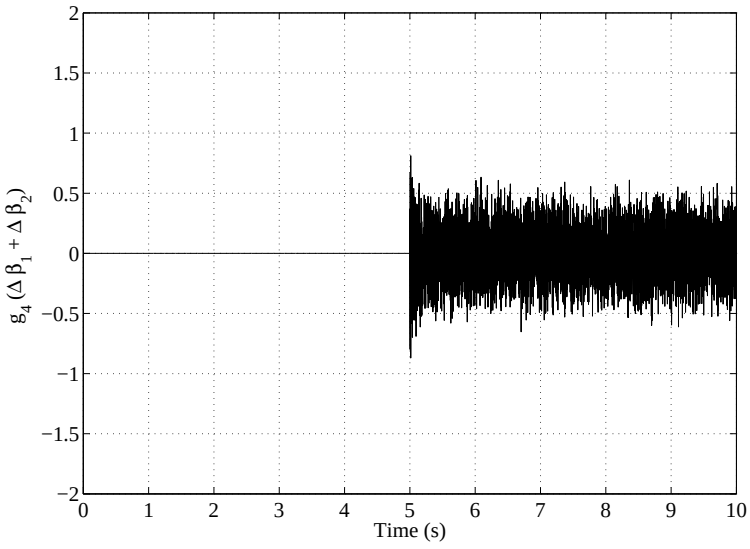

Fig. 7 The combined control input disturbance

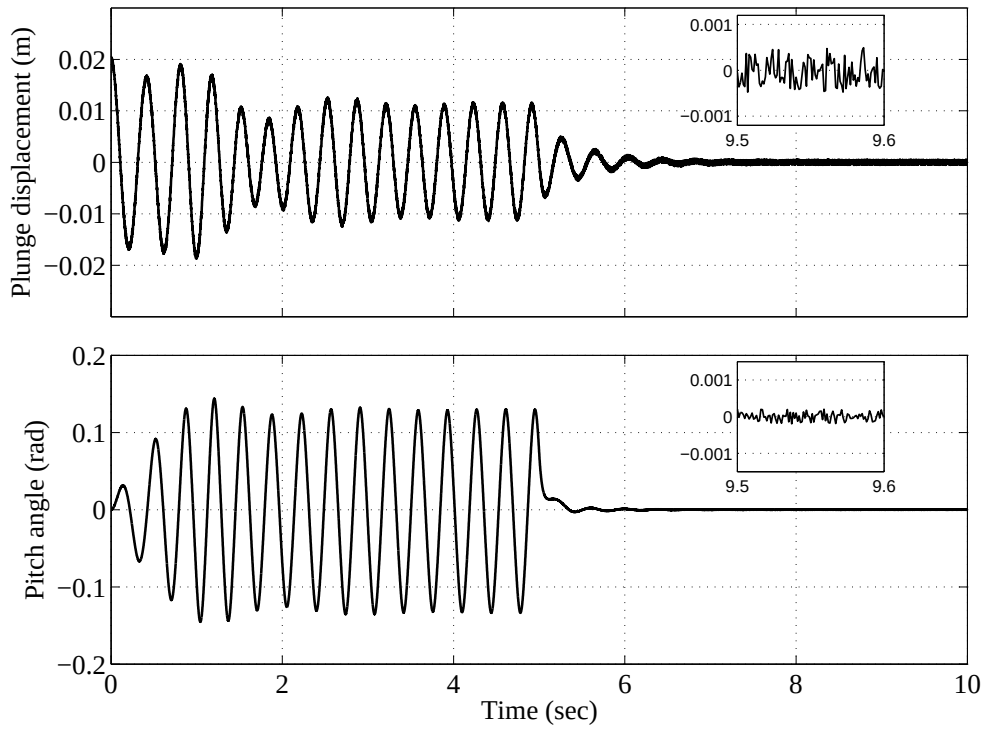

Fig. 8 Time histories of plunge displacement and pitch angle - nonlinear pitch stiffness uncertainty and random primary and secondary input disturbances

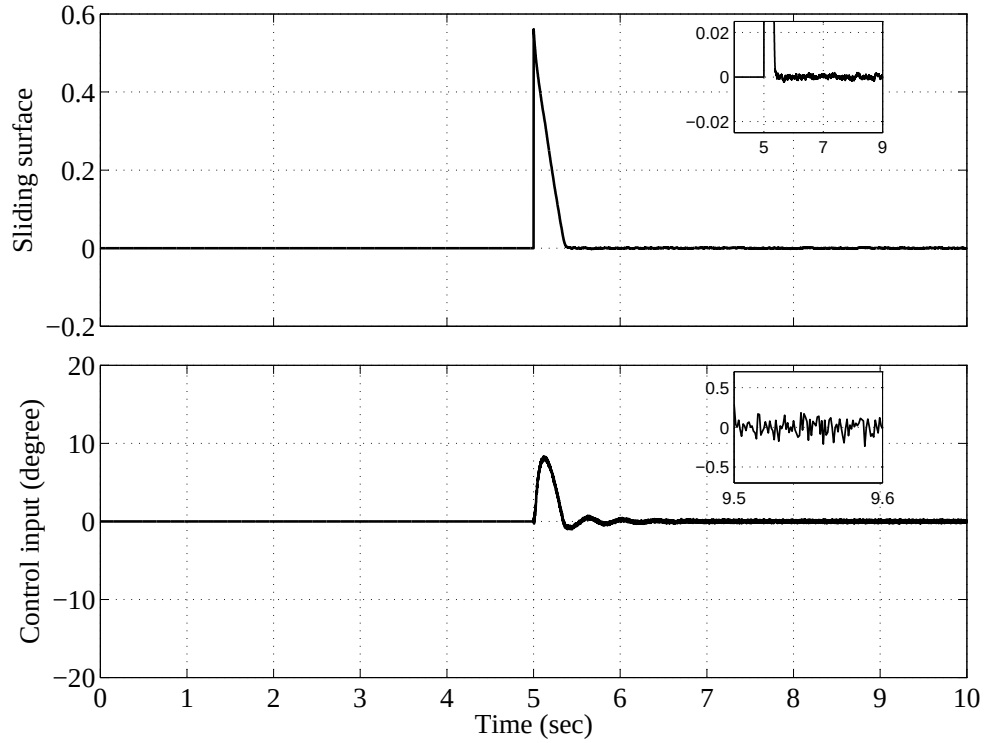

Fig. 9 Sliding surface and trailing edge control surface angle - nonlinear pitch stiffness uncertainty and random primary and secondary input disturbances

6. Conclusions

A new approach is developed for the suppression of flutter instability in an under-actuated prototypical wing section with torsional nonlinearity. Robust passivity-based control is used to design a nonlinear sliding-mode surface in the presence of matched and unmatched uncertainty and input disturbance. A continuous sliding-mode control input is employed to stabilise the overall system. With known bounded input disturbance and nonlinearity uncertainty, the controller is able in theory to globally stabilise the overall system when the zero dynamics are globally exponentially stable. In the presence of practical limits on the actuator flap deflection, as represented in a numerical case study, the controlled system is shown to be stable in the local sense.

Acknowledgement: The work described in this paper forms part of a research programme funded by EPSRC under grant EP/J0049871/1. The first author acknowledges the support of a Chinese Scholarship Council award and a studentship from the University of Liverpool.

Appendix 1: Expressions for $\Phi_1\left(\mathbf{z}_{(1-3)}\right)$ and $\Phi_2(\mathbf{z})$

$\Phi_1\left(\mathbf{z}_{(1-3)}\right)$ may be determined using (15), (26) and (29) as,

$$\begin{aligned}\Phi_1\left(\mathbf{z}_{(1-3)}\right) &= -\frac{dW\left(\mathbf{z}_{(1-2)}\right)}{d\mathbf{z}_{(1-2)}}\mathbf{f}_2 - \frac{1}{2\lambda}n^2(z_3)z_3 - \chi z_3 = -2\mathbf{z}_{(1-2)}^T\mathbf{P}\mathbf{f}_2 - \frac{1}{2\lambda}n^2(z_3)z_3 - \chi z_3 \\ &= -\left[\left(\frac{\varphi_1 q_2}{\varphi_2\varphi_4^2} - \frac{q_1}{\varphi_2}\right)\varphi_4 - \frac{q_1}{\varphi_1}\left(\varphi_{31} + \varphi_{32}K_\alpha(z_3)\right)\right]z_1 \\ &\quad -\left[q_2 + \left(\frac{q_2}{\varphi_2\varphi_4} - \frac{\varphi_4 q_1}{\varphi_1\varphi_2}\right)\left(\varphi_{31} + \varphi_{32}K_\alpha(z_3)\right)\right]z_2 - \frac{1}{2\lambda}n^2(z_3)z_3 - \chi z_3\end{aligned} \tag{69}$$

while $\Phi_2(\mathbf{z})$, using (14)-(17), (48) and (69), may be expressed as,

$$\begin{aligned}\Phi_2(\mathbf{z}) &= \varphi_7 z_1 + \varphi_4\varphi_8(z_3 - z_2) + \varphi_{91}z_3 + \varphi_{92}K_\alpha(z_3)z_3 + \varphi_{10}z_4 \\ &\quad + \left[\left(\frac{\varphi_1 q_2}{\varphi_2\varphi_4^2} - \frac{q_1}{\varphi_2}\right)\varphi_4 - \frac{q_1}{\varphi_1}\left(\varphi_{31} + \varphi_{32}K_\alpha(z_3)\right)\right]\varphi_4(z_3 - z_2) \\ &\quad + \left[q_2 + \left(\frac{q_2}{\varphi_2\varphi_4} - \frac{\varphi_4 q_1}{\varphi_1\varphi_2}\right)\left(\varphi_{31} + \varphi_{32}K_\alpha(z_3)\right)\right] \\ &\quad \times\left(-\frac{1}{\varphi_4}\right)\left[\varphi_1 z_1 + \varphi_4\varphi_2(z_3 - z_2) + \varphi_{31}z_3 + \varphi_{32}K_\alpha(z_3)z_3\right] \\ &\quad + \left[-\frac{\varphi_{32}q_1}{\varphi_1}z_1 + \varphi_{32}\left(\frac{q_2}{\varphi_2\varphi_4} - \frac{\varphi_4 q_1}{\varphi_1\varphi_2}\right)z_2\right]\frac{\partial K_\alpha(z_3)}{\partial z_3}z_4 + \chi z_4 + \frac{1}{2\lambda}\frac{\partial\left(n^2(z_3)z_3\right)}{\partial z_3}z_4\end{aligned} \tag{70}$$

Appendix 2: Continuous sliding-mode control design.

The motion during continuous sliding-mode control generally consists only of a *reaching phase*, during which trajectories, starting away from the sliding surface $s = 0$, move towards it and are then confined to a thin boundary layer close to it. There is generally no sliding phase because the states never reach the sliding surface exactly.

In the reaching phase, i.e., $s = z_4 - \Phi_1\left(\mathbf{z}_{(1-3)}\right) \neq 0$, the system (11)-(12) becomes,

$$\dot{\mathbf{z}}_{(1-2)} = \mathbf{f}_1\left(\mathbf{z}_{(1-2)}\right) + \mathbf{f}_2\left(\mathbf{z}_{(1-3)}\right) z_3 + \boldsymbol{\delta}_1 \tag{71}$$

$$\dot{z}_3 = \Phi_1\left(\mathbf{z}_{(1-3)}\right) + s \tag{72}$$

Equations (71)-(72) define a reduced order system with s viewed as input. The saturation function in equation (57) allows the behaviour under two different input levels, outside the boundary layer $\left(|s| > \varepsilon\right)$ and inside the boundary layer $\left(|s| \leq \varepsilon\right)$, to be considered separately.

Outside the boundary layer, $|s| > \varepsilon$:

The substitution of equation (57) into (50) leads to,

$$\dot{U}_2 = s\Phi_3\left(\mathbf{z}\right)\Delta K_\alpha\left(z_3\right) z_3 - s\xi\left(\mathbf{z}\right)\mathrm{sat}\left(\frac{s}{\varepsilon}\right) + sg_4\Delta\beta - s\xi_1\mathrm{sat}\left(\frac{s}{\varepsilon}\right) - \upsilon s^2 \tag{73}$$

Then by combining this expression with the inequalities(53), (54) and (56) it is found that,

$$\dot{U}_2 \leq -\left(1-\eta_0\right)\xi_0|s| - \left(1-\eta_1\right)\xi_1|s| - \upsilon s^2 \leq 0 \tag{74}$$

Inequality (74) implies that whenever $|s(0)| > \varepsilon$, $|s(t)|$ will decrease until it reaches in the boundary layer $\left(|s| \leq \varepsilon\right)$ and afterwards remain there. The boundary layer $\left(|s| \leq \varepsilon\right)$ is a positively invariant set.

Inside the boundary layer, $|s| \leq \varepsilon$:

The behaviour of the overall closed-loop system can be further examined by investigating the behaviour of the system (71)-(72) with s, $|s| \leq \varepsilon$, viewed as the input.

Taking $U_1\left(\mathbf{z}_{(1-3)}\right)$ given by (37) as a Lyapunov function candidate for the system (71)-(72),

$$\dot{U}_1 = \frac{\mathrm{d}U_1}{\mathrm{d}\mathbf{z}_{(1-3)}}\dot{\mathbf{z}}_{(1-3)} = \begin{bmatrix} \dfrac{\mathrm{d}W\left(\mathbf{z}_{(1-2)}\right)}{\mathrm{d}\mathbf{z}_{(1-2)}} & z_3 \end{bmatrix} \begin{bmatrix} \dot{\mathbf{z}}_{(1-2)} \\ \dot{z}_3 \end{bmatrix} \tag{75}$$

combining with equations (71)-(72),

$$\dot{U}_1 = \frac{\mathrm{d}W\left(\mathbf{z}_{(1-2)}\right)}{\mathrm{d}\mathbf{z}_{(1-2)}}\mathbf{f}_1 + z_3\frac{\mathrm{d}W\left(\mathbf{z}_{(1-2)}\right)}{\mathrm{d}\mathbf{z}_{(1-2)}}\mathbf{f}_2 + \frac{\mathrm{d}W\left(\mathbf{z}_{(1-2)}\right)}{\mathrm{d}\mathbf{z}_{(1-2)}}\boldsymbol{\delta}_1 + z_3\boldsymbol{\Phi}_1\left(\mathbf{z}_{(1-3)}\right) + z_3 s \tag{76}$$

and with (6), (36) and (42) leads to,

$$\begin{aligned}\dot{U}_1 &\le \frac{\mathrm{d}W\left(\mathbf{z}_{(1-2)}\right)}{\mathrm{d}\mathbf{z}_{(1-2)}}\mathbf{f}_1 + \left|\frac{dW\left(\mathbf{z}_{(1-2)}\right)}{d\mathbf{z}_{(1-2)}}\tilde{\mathbf{t}}\right|\left|\Delta K_\alpha\left(z_3\right)z_3\right| - \frac{1}{2\lambda}n^2\left(z_3\right)z_3^2 - \chi z_3^2 + z_3 s \\ &\le \frac{\mathrm{d}W\left(\mathbf{z}_{(1-2)}\right)}{\mathrm{d}\mathbf{z}_{(1-2)}}\mathbf{f}_1 + \left|\frac{dW\left(\mathbf{z}_{(1-2)}\right)}{d\mathbf{z}_{(1-2)}}\tilde{\mathbf{t}}\right|\left|n\left(z_3\right)z_3\right| - \frac{1}{2\lambda}n^2\left(z_3\right)z_3^2 - \chi z_3^2 + z_3 s \\ &\le \frac{\mathrm{d}W\left(\mathbf{z}_{(1-2)}\right)}{\mathrm{d}\mathbf{z}_{(1-2)}}\mathbf{f}_1 + \frac{\lambda}{2}\left(\frac{dW\left(\mathbf{z}_{(1-2)}\right)}{d\mathbf{z}_{(1-2)}}\tilde{\mathbf{t}}\right)^2 - \chi z_3^2 + z_3 s\end{aligned} \tag{77}$$

Now, introducing the inequality(35),

$$\dot{U}_1 \le -\gamma_1\left\|\mathbf{z}_{(1-2)}\right\|_2^2 - \chi z_3^2 + \left|z_3\right|\left|s\right| \tag{78}$$

and separating $-\gamma_1\left\|\mathbf{z}_{(1-2)}\right\|_2^2$ into three parts, $-(1-\varsigma)\gamma_1\left\|\mathbf{z}_{(1-2)}\right\|_2^2$, $-\frac{\varsigma}{2}\gamma_1\left\|\mathbf{z}_{(1-2)}\right\|_2^2$ and $-\frac{\varsigma}{2}\gamma_1\left\|\mathbf{z}_{(1-2)}\right\|_2^2$, and χz_3^2 into two parts, $\chi(1-\mu)z_3^2$ and $\chi\mu z_3^2$, then,

$$\begin{aligned}\dot{U}_1 \le &-(1-\varsigma)\gamma_1\left\|\mathbf{z}_{(1-2)}\right\|_2^2 - \frac{\varsigma}{2}\gamma_1\left\|\mathbf{z}_{(1-2)}\right\|_2^2 - \frac{\varsigma}{2}\gamma_1\left\|\mathbf{z}_{(1-2)}\right\|_2^2 \\ &-\chi(1-\mu)z_3^2 - \chi\mu z_3^2 + \left|z_3\right|\left|s\right|\end{aligned} \tag{79}$$

where $0 < \varsigma, \mu < 1$.

It is readily seen that $\left|z_1\right| \le \left\|\mathbf{z}_{(1-2)}\right\|_2^2$ and $\left|z_2\right| \le \left\|\mathbf{z}_{(1-2)}\right\|_2^2$, in which case,

$$\dot{U}_1 \le -(1-\varsigma)\gamma_1\left\|\mathbf{z}_{(1-2)}\right\|_2^2 - \chi(1-\mu)z_3^2 - \frac{\varsigma}{2}\gamma_1\left|z_1\right| - \frac{\varsigma}{2}\gamma_1\left|z_2\right| - \chi\mu z_3^2 + \left|z_3\right|\left|s\right| \tag{80}$$

If $\left|s\right|/(\chi\mu) < \left|z_3\right|$, such that,

$$-\chi\mu z_3^2 + \left|z_3\right|\left|s\right| < 0 \tag{81}$$

then,

$$\begin{aligned}\dot{U}_1 &\le -(1-\varsigma)\gamma_1\left\|\mathbf{z}_{(1-2)}\right\|_2^2 - \chi(1-\mu)z_3^2 - \frac{\varsigma}{2}\gamma_1|z_1| - \frac{\varsigma}{2}\gamma_1|z_2| \\ &\le -(1-\varsigma)\gamma_1\left\|\mathbf{z}_{(1-2)}\right\|_2^2 - \chi(1-\mu)z_3^2 \\ &\le -\min\left((1-\varsigma)\gamma_1, \chi(1-\mu)\right)\left\|\mathbf{z}_{(1-3)}\right\|_2^2 \\ &\le 0\end{aligned} \tag{82}$$

Also, if

$$|z_3| \le |s|/(\chi\mu) \quad \text{and} \quad 2|s|^2/(\varsigma\chi\mu\gamma_1) \le |z_1| \tag{83}$$

or,

$$|z_3| \le |s|/(\chi\mu) \quad \text{and} \quad 2|s|^2/(\varsigma\chi\mu\gamma_1) \le |z_2| \tag{84}$$

then,

$$-\frac{\varsigma}{2}\gamma_1|z_1| + |z_3||s| \le 0 \ \text{ or } \ -\frac{\varsigma}{2}\gamma_1|z_2| + |z_3||s| \le 0 \tag{85}$$

and,

$$\begin{aligned}\dot{U}_1 &\le -(1-\varsigma)\gamma_1\left\|\mathbf{z}_{(1-2)}\right\|_2^2 - \chi(1-\mu)z_3^2 - \chi\mu z_3^2 \\ &\le -(1-\varsigma)\gamma_1\left\|\mathbf{z}_{(1-2)}\right\|_2^2 - \chi(1-\mu)z_3^2 \\ &\le -\min\left((1-\varsigma)\gamma_1, \chi(1-\mu)\right)\left\|\mathbf{z}_{(1-3)}\right\|_2^2 \\ &\le 0\end{aligned} \tag{86}$$

By combining the conditions (81), (83) and (84) on the inequality (82) and (86), the dynamics of the system is found to be stable under the single condition that there exists a positive real number γ_3 such that,

$$\gamma_3\left\|\mathbf{z}_{(1-3)}\right\|_2 \ge \left\|\mathbf{z}_{(1-3)}\right\|_\infty \ge \kappa(|s|) = \max\left\{|s|/(\chi\mu),\ 2|s|^2/(\varsigma\chi\mu\gamma_1)\right\},\ \forall\mathbf{z}_{(1-3)} \in R^{3\times 1} \tag{87}$$

where $\|(\bullet)\|_\infty$ is the infinity norm of $(\bullet)$ and $\forall\mathbf{z}_{(1-3)} \in R^{3\times 1}$. It can be seen that $\kappa(|s|)$ a strictly increasing function of $|s|$ with $\kappa(0) = 0$.

Then by invoking Theorem 4.19 [28] with inequalities (38), (82), (86) and (87) the subsystem (71)-(72) is found to be input-to-state stable so that the states are bounded under bounded input.

Lemma A2.1 Consider the system (11)-(12). Suppose the zero dynamics $\dot{\mathbf{z}} = \mathbf{f}_1(\mathbf{z}) = \mathbf{S}\mathbf{z}$ are globally exponentially stable and inequalities (6), (53) and (54) are satisfied. Then using the

continuous sliding-mode controller (57), the trajectory of the full closed-loop system will be bounded for all $t \geq 0$ and reaches a positively invariant set (92) controlled by the design parameter ε. Moreover, if $\eta(\mathbf{0}) = 0$, $\eta_0 = 0$ and $\Delta\beta = 0$, then there exists $\varepsilon^* > 0$ such that for all $0 < \varepsilon < \varepsilon^*$, the origin of the full closed-loop system will be globally asymptotically stable.

Proof: The preceding analysis shows that whenever $|s(0)| > \varepsilon$, $|s(t)|$ will decrease until it reaches the boundary layer $(|s| \leq \varepsilon)$ and remain inside thereafter. The boundary layer is a positively invariant set $\{|s| \leq \varepsilon\}$.

Recalling that $\kappa(|s|)$ is a strictly increasing function of $|s|$, we now choose $|s| = \varepsilon$ as the upper limit of $|s|$ within the boundary layer. Then U_3 may be introduced as a strictly increasing function of ε as,

$$U_3(\varepsilon) = \max\left(\lambda_{\max}(\mathbf{P}), \frac{1}{2}\right)\left(\frac{1}{\gamma_3}\kappa(\varepsilon)\right)^2 \tag{88}$$

where $|s| \leq \varepsilon$.

Let us assume that $U_1\left(\mathbf{z}_{(1-3)}\right) \geq U_3(\varepsilon)$. Then by combining (38) and (88) it is found that,

$$U_3(\varepsilon) = \max\left(\lambda_{\max}(\mathbf{P}), \frac{1}{2}\right)\left(\frac{1}{\gamma_3}\kappa(\varepsilon)\right)^2 \leq U_1\left(\mathbf{z}_{(1-3)}\right) \leq \max\left(\lambda_{\max}(\mathbf{P}), \frac{1}{2}\right)\left\|\mathbf{z}_{(1-3)}\right\|_2^2 \tag{89}$$

which means that,

$$\frac{1}{\gamma_3}\kappa(\varepsilon) \leq \left\|\mathbf{z}_{(1-3)}\right\|_2 \tag{90}$$

Since $|s| \leq \varepsilon$, inequality (90) becomes,

$$\left\|\mathbf{z}_{(1-3)}\right\|_2 \geq \frac{1}{\gamma_3}\kappa(\varepsilon) \geq \frac{1}{\gamma_3}\kappa(|s|) \tag{91}$$

This result confirms the inequality (87). Thus, inside the boundary layer, if $\left\{U_1\left(z_{(1-3)}\right) \geq U_3(\varepsilon)\right\}$, then $\dot{U}_1 \leq 0$, so that the system is globally stable under the condition,

$$\Omega_\varepsilon = \left\{U_1\left(\mathbf{z}_{(1-3)}\right) \leq U_3(\varepsilon)\right\} \cap \{|s| \leq \varepsilon\} \tag{92}$$

where $\cap$ denotes the intersection.

Thus, whenever $|s(0)| > \varepsilon$, $|s(t)|$ will decrease until it reaches the boundary layer $(|s| \le \varepsilon)$ and afterwards remain there. Eventually, the trajectory of the full closed-loop system is found to be bounded for all $t \ge 0$ and reaches a positively invariant set (92) controlled by the design parameter ε. Moreover, the system (11)-(12) with $z_4 = \Phi_3\left(\mathbf{z}_{(1-3)}\right)$ is globally exponentially stable. If $\eta(\mathbf{0}) = 0$, $\eta_0 = 0$ and $\Delta\beta = 0$, then according to Theorem 14.2 [28], there exists ε^* such that for all $0 < \varepsilon < \varepsilon^*$, the origin of the full closed-loop system will be globally asymptotically stable.

□

References

[1] C.M. Denegri, Limit cycle oscillation flight test results of a fighter with external stores, Journal of Aircraft, 37 (2000) 761-769.
[2] R.W. Bunton, C.M. Denegri Jr, Limit cycle oscillation characteristics of fighter aircraft, Journal of Aircraft, 37 (2000) 916-918.
[3] L. Trame, L. Williams, R. Yurkovich, Active aeroelastic oscillation control on the F/A-18 aircraft, Guidance, Navigation and Control Conference, American Institute of Aeronautics and Astronautics1985.
[4] P.M. Hartwich, S.K. Dobbs, A.E. Arslan, S.C. Kim, Navier-Stokes computations of limit-cycle oscillations for a B-1-like configuration, Journal of Aircraft, 38 (2001) 239-247.
[5] S. Jacobson, R. Britt, D. Freim, P. Kelly, Residual pitch oscillation (RPO) flight test and analysis on the B-2 bomber, 39th AIAA/ASME/ASCE/AHS/ASC Structures, Structural Dynamics, and Materials Conference and Exhibit, American Institute of Aeronautics and Astronautics1998.
[6] J. Croft, Airbus elevator flutter: Annoying or dangerous?, Aviation Week & Space Technology, 155 (2001) 41.
[7] L. Librescu, G. Chiocchia, P. Marzocca, Implications of cubic physical/aerodynamic non-linearities on the character of the flutter instability boundary, International Journal of Non-Linear Mechanics, 38 (2003) 173-199.
[8] J.S. Vipperman, J.M. Barker, R.L. Clark, G.J. Balas, Comparison of mu- and H2-Synthesis Controllers on an experimental typical section, Journal of Guidance, Control, and Dynamics, 22 (1999) 278-285.
[9] L. Yang, Y. Hongnian, H. Yu, Y. Liu, A survey of underactuated mechanical systems, IET Control Theory & Applications, 7 (2013) 921-935.
[10] X. Wei, J.E. Mottershead, Limit cycle assignment in nonlinear aeroelastic systems using describing functions and the receptance method, in: R. Allemang, J. De Clerck, C. Niezrecki, A. Wicks (Eds.) Topics in Modal Analysis, Volume 7: Proceedings of the 31st IMAC, A Conference on Structural Dynamics, 2013, Springer, New York, 2014, pp. 701-713..
[11] J.J. Block, T.W. Strganac, Applied active control for a nonlinear aeroelasticstructure, Journal of Guidance, Control, and Dynamics, 21 (1998) 838-845.
[12] K.D. Frampton, R.L. Clark, Experiments on Control of Limit-Cycle Oscillations in a Typical Section, Journal of Guidance, Control, and Dynamics, 23 (2000) 956-960.
[13] J. Ko, A.J. Kurdila, T.W. Strganac, Nonlinear control of a prototypical wing section with torsional nonlinearity, Journal of Guidance, Control, and Dynamics, 20 (1997) 1181-1189.
[14] J.W. Ko, T.W. Strganac, A.J. Kurdila, Stability and control of a structurally nonlinear aeroelastic system, Journal of Guidance Control and Dynamics, 21 (1998) 718-725.
[15] J. Ko, T.W. Strganac, A.J. Kurdila, Adaptive feedback linearization for the control of a typical wing section with structural nonlinearity, Nonlinear Dynamics, 18 (1999) 289.
[16] J. Ko, T.W. Strganac, J.L. Junkins, M.R. Akella, A.J. Kurdila, Structured model reference adaptive control for a wing section with structural nonlinearity, Journal of Vibration and Control, 8 (2002) 553-573.

[17] A. Behal, P. Marzocca, V.M. Rao, A. Gnann, Nonlinear adaptive control of an aeroelastic two-dimensional lifting surface, Journal of Guidance, Control, and Dynamics, 29 (2006) 382.
[18] W. Xing, S.N. Singh, Adaptive output feedback control of a nonlinear aeroelastic structure, Journal of Guidance, Control, and Dynamics, 23 (2000) 1109-1116.
[19] K.W. Lee, S.N. Singh, Global robust control of an aeroelastic system using output feedback, Journal of Guidance, Control, and Dynamics, 30 (2007) 271-275.
[20] F. Zhang, D. Soffker, Active flutter suppression of a nonlinear aeroelastic system using PI-observer, in: H. Ulbrich, L. Ginzinger (Eds.) Motion and Vibration Control, Springer Netherlands2009, pp. 367-376.
[21] T. Degaki, S. Suzuki, Sliding mode control application for two-dimensional active flutter suppression, Transactions of the Japan Society for Aeronautical and Space Sciences, 43 (2001) 174-181.
[22] C.L. Chen, C.C. Peng, H.T. Yau, High-order sliding mode controller with backstepping design for aeroelastic systems, Communications in Nonlinear Science and Numerical Simulation, 17 (2012) 1813-1823.
[23] K.W. Lee, S.N. Singh, Robust higher-order sliding-mode finite-time control of aeroelastic systems, Journal of Guidance, Control, and Dynamics, 37 (2014) 1664-1671.
[24] C. Chieh-Li, C. Chung-Wei, Y. Her-Terng, Design of dynamic sliding mode controller to aeroelastic systems, Applied Mathematics & Information Sciences, 6 (2012) 89-98.
[25] B.-H. Lee, J.-h. Choo, S. Na, P. Marzocca, L. Librescu, Sliding mode robust control of supersonic three degrees-of-freedom airfoils, International Journal of Control, Automation and Systems, 8 (2010) 279-288.
[26] S. Gujjula, S.N. Singh, Variable structure control of unsteady aeroelastic system with partial state information, Journal of Guidance, Control, and Dynamics, 28 (2005) 568-573.
[27] R. Xu, Ü. Özgüner, Sliding mode control of a class of underactuated systems, Automatica, 44 (2008) 233-241.
[28] H.K. Khalil, Nonlinear systems, Upper Saddle River, N.J. : Prentice Hall2002.
[29] Y.C. Fung, An introduction to the theory of aeroelasticity, Wiley, New York, 1955.
[30] W. Lin, T. Shen, Robust passivity and feedback design for minimum-phase nonlinear systems with structureal uncertainty, Automatica, 35 (1999) 35-47.
[31] C.I. Byrnes, A. Isidori, J.C. Willems, Passivity, feedback equivalence, and the global stabilization of minimum phase nonlinear systems, Automatic Control, IEEE Transactions on, 36 (1991) 1228-1240.
[32] K.D. Young, V.I. Utkin, U. Ozguner, A control engineer's guide to sliding mode control, IEEE Transactions on Control Systems Technology, 7 (1999) 328-342.